REPORT DOCUMENTATION PAGE

Form Approved
OMB No. 0704-0188

1. AGENCY USE ONLY (Leave blank)	2. REPORT DATE	3. REPORT TYPE AND DATES COVERED
	29 June 1995	Annual Summary 1 June 94 - 31 May 95

4. TITLE AND SUBTITLE
SCATTERING AND RADIATION OF HIGH FREQUENCY SOUND IN WATER BY ELASTIC OBJECTS, PARTICLE SUSPENSIONS, AND CURVED SURFACES

5. FUNDING NUMBERS
PE 61153N
G N0001492J1600
TA 3126960

6. AUTHOR(S)
Philip L. Marston

7. PERFORMING ORGANIZATION NAME(S) AND ADDRESS(ES)
Department of Physics
Washington State University
Pullman, WA 99164-2814

8. PERFORMING ORGANIZATION REPORT NUMBER
N00014-92-J-1600-AR2

9. SPONSORING / MONITORING AGENCY NAME(S) AND ADDRESS(ES)
Office of Naval Research - ONR 331
800 North Quincy Street
Arlington, VA 22217-5660

10. SPONSORING / MONITORING AGENCY REPORT NUMBER

11. SUPPLEMENTARY NOTES
Research proposed in "Geometrical and Surface Aspects of Scattering and Nonlinear Acoustics," and in AASERT proposal, P. L. Marston, principal investigator. Telephone (509) 335-5343

12a. DISTRIBUTION / AVAILABILITY STATEMENT
Approved for public release: Distribution unlimited

12b. DISTRIBUTION CODE

13. ABSTRACT *(Maximum 200 words)*

The research reported is principally in the areas: (A) Scattering of high-frequency sound or pressure impulses by elastic objects in water--Experiments and theory are examined for scattering of pressure impulses and high-frequency sound by elastic objects in water. Improved capability for measuring the impulse response is discussed and examples given include: (1) the bipolar specular feature that reveals the mass-per-area of the shell; (2) the beating of low frequency flexural modes of a shell; and (3) the impulse response of a thick cylindrical shell. Other measurements include retro-reflective backscattering due to Rayleigh waves on objects with corners. Research includes a convolution formulation for objects having variable curvature or truncations and an analysis of the background phase for shells. (B) Wavefields of random caustics produced by reflection--Wavefields were measured for reflection from a randomly corrugated pressure-release surface in water for a range of frequencies of the incident pulse. The resulting wavefields and intensity moments were modeled with catastrophe theory which accounts for the fluctuations due to caustics. Intensity moments greater than the second were proportional to the frequency raised to an exponent (the twinkling exponent). (C) Interaction of sound with sound mediated by a suspension of particles was demonstrated with the probe wave collinear with the standing pump wave.

14. SUBJECT TERMS	15. NUMBER OF PAGES
Acoustical Scattering, Ray Methods, Elastic Shells, Evanescent Waves, Plates, Particle Suspensions, Nonlinear Acoustics, Rayleigh Waves	35
	16. PRICE CODE

17. SECURITY CLASSIFICATION OF REPORT	18. SECURITY CLASSIFICATION OF THIS PAGE	19. SECURITY CLASSIFICATION OF ABSTRACT	20. LIMITATION OF ABSTRACT
UNCLASSIFIED	UNCLASSIFIED	UNCLASSIFIED	

SCATTERING AND RADIATION OF HIGH FREQUENCY SOUND IN WATER BY ELASTIC OBJECTS, PARTICLE SUSPENSIONS, AND CURVED SURFACES

Philip L. Marston
Department of Physics
Washington State University
Pullman, Washington 99164-2814

June 1995

Annual Summary Report for Grant N00014-92-J-1600

1 June 1994 - 31 May 1995

Approved for public release: Distribution Unlimited.

Prepared for: **Office of Naval Research**
Chemistry and Physics S & T Division (ONR 331)
800 North Quincy Street
Arlington, VA 22217-5660

ABSTRACT

Research in the following areas is reported in this Annual Summary Report:

A. **Scattering of high-frequency sound or pressure impulses by elastic objects in water**--Experiments and theory are examined for scattering of pressure impulses and high-frequency tone bursts by elastic objects in water. Improved capability for measuring the impulse response is discussed and examples are given including: (i) the bipolar specular feature that reveals the mass-per-area of the shell; (ii) the beating of low frequency flexural modes of a shell; and (iii) the impulse response of a thick cylindrical shell. Thick shell dispersion and radiation damping curves display qualitative differences with thin shell results relevant to our measurements. Other measurements include retro-reflective backscattering of tone bursts due to Rayleigh waves on objects with corners. Theoretical advances include a convolution formulation of leaky wave contributions to scattering for objects having variable curvature or truncations and analysis of the phase of background contributions to backscattering by thick and thin shells.

B. **Wavefields of random caustics produced by reflection: Measurements of intensity moments and twinkling exponents**--Wavefields were measured for reflection from a randomly corrugated pressure-release surface in water for a range of frequencies of the incident pulse. The resulting wavefields and intensity moments were modeled with catastrophe theory which accounts for the fluctuations due to caustics. The intensity moments greater than the second were proportional to the frequency raised to an exponent (M. V. Berry's "twinkling exponent").

C. **Interaction of sound with sound mediated by a suspension of particles**--A new measurement configuration was demonstrated where the ultrasonic probe wave is collinear with the standing pump ultrasonic wave.

D. **Supplemental research: Light scattering and sonoluminescence**--Publications pertaining to light scattering are noted as well as aspects of the optical modes of bubbles and single bubble sonoluminescence.

TABLE OF CONTENTS

I. RESEARCH PROJECTS

This section summarizes the research results in the context of previous work by others and by Marston and associates. The reader should see the various publications and reports referenced for theoretical and technical details. The publications give additional references to the broader scientific literature and are listed in Section III. Most of the work previously submitted for publication and published during this year was described in last year's Report.[T3] Some of that research will be reviewed when needed to introduce the current research.

A. Scattering of high-frequency sound or pressure impulses by elastic objects in water.

This research program has examined high-frequency scattering situations where the elastic contributions to backscattering are large. For situations where the scatterer is an elastic shell, various elastic responses of interest include waves not describable by theories for scattering by thin shells being developed by other researchers. Thus, for example, it is usually necessary to rely on dispersion relations based on the full equations of elasticity with fluid loading (instead of the much simpler equations of a fluid-loaded "thin shell"). Examples of pronounced coupling processes included backwards (or negative group velocity) waves[J6] and coincidence frequency enhancements[J7,J9] occurring near frequency thresholds for coupling. Kaduchak's Ph.D. dissertation[T1] (some of which he had previously published) gives an experimental study of such processes. The dissertation abstract is given as **Figure 1.** Another unique aspect of our investigation is the response of shells to pressure impulses of extremely broad spectral content as summarized in Sections A1-3. The high-frequency content for some of the scattering processes of interest may preclude the description of scattering features by various numerical algorithms based on discretized descriptions of the structure being developed by other programs. Potential applications are not limited to underwater acoustics but also include ultrasonic testing.

1. Source of plane wave pressure impulses for scattering experiments: Analysis and testing.

A new transducer configuration was developed with the support of this grant for the measurement of the response of a target to a plane wave impulse.[J9,T3] The source consisted of a large sheet of PVDF piezoelectric polymer with water in contact with both sides. This year Scot Morse improved the source and the spectrum of the pressure impulse was modeled.[M12] The improvements include: (a) a high current FET pulse generator to

Mode threshold and transient scattering processes for high-frequency scattering of sound by elastic shells in water [43.20.Fn, 43.20.Px, 43.40.Rj]—Gregory Kaduchak, *Department of Physics, Washington State University, Pullman, WA 99164-2814, August 1994 (Ph.D.).* Large backscattering enhancements associated with threshold frequencies of guided waves launched on empty spherical and cylindrical shells in water are investigated. These include the subsonic a_{0-} Lamb wave responsible for large backscattered signatures in the low- and coincidence-frequency regions on empty and fluid-filled shells and the "negative" group velocity s_{2b} Lamb wave responsible for a large, prompt echo return near the first thickness resonance. The large s_{2b} backward wave contribution does not require propagation around the "shadow" or backside of the shell. Thus it is only affected by shell properties closest to the source. Tone-burst experiments confirm prediction of quantitative ray acoustic approximations based on full elasticity theory. The work presented here is beyond the scope of quantitative ray methods for shells based on thin shell theory. Thin shell approximations do not properly describe the dispersion relations near the coincidence frequency for metallic objects in water or higher order Lamb modes such as the s_{2b} Lamb wave. For the scattering processes the associated echo amplitudes may be over five times the amplitude of the specular reflection. Broadband transient experiments were performed with a newly developed pressure source. It consists of a PVDF sheet in contact with water on both sides and yields a near-field pressure impulse when driven by a step voltage. The source is nonconventional in the sense that the backscattered echoes travel through the source to a far-field receiver. Prominent features of the shell's impulse response are observed over a frequency interval which includes both low- and coincidence-frequency excitations and the bipolar nature of the specular reflection. The latter property is modeled with shell theory and contains information about the mass-per-area of the shell. Some computational aspects concern a_{0-} and s_{2b} guided wave surface displacements on cylindrical shells and the $a_{\dot{0}-}$ backscattering contribution for a shell filed with water.

Thesis advisor: Philip L. Marston.

Figure 1

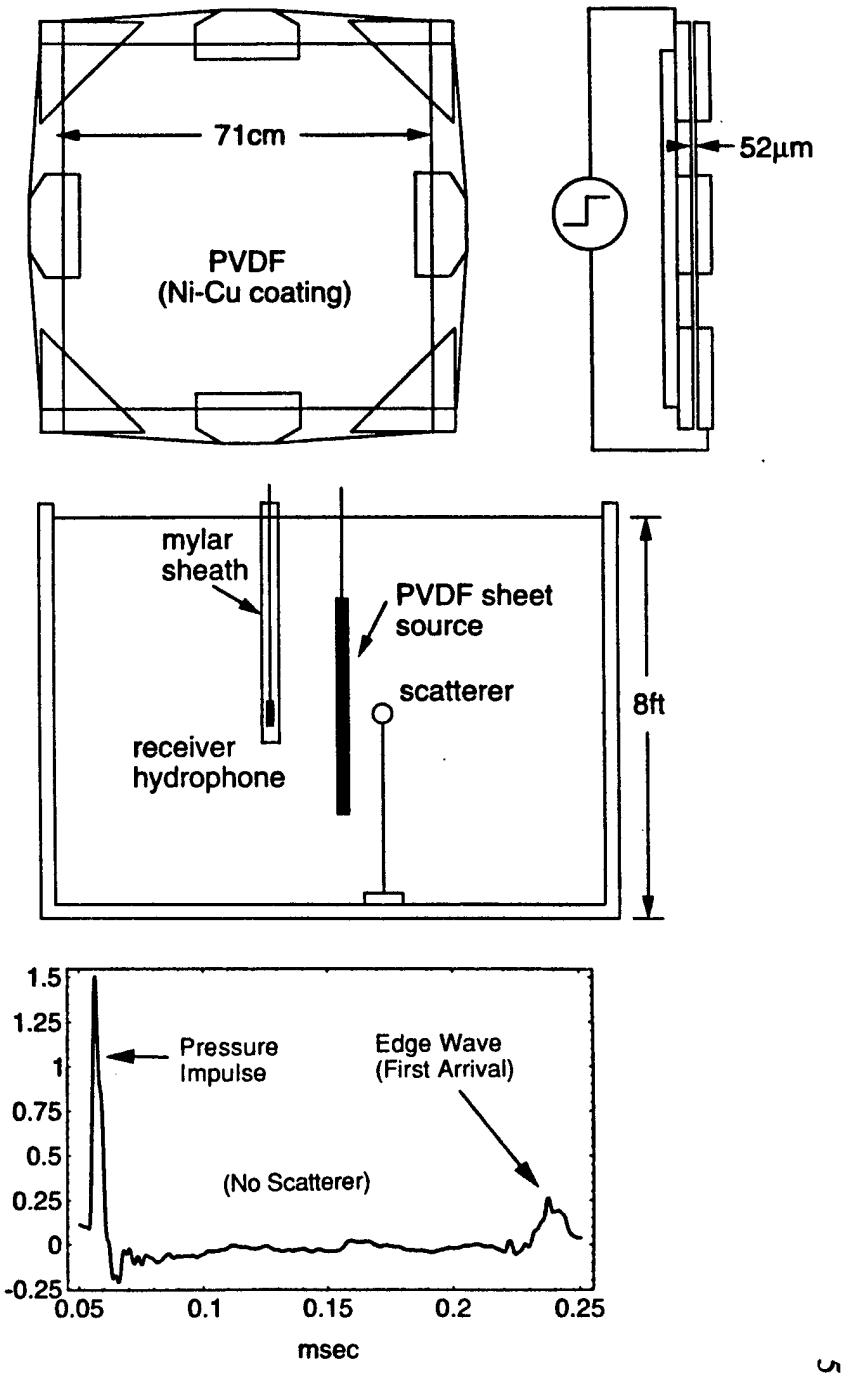

Figure 2

drive the PVDF and other improvements that reduce spurious electrical coupling to the hydrophone and (b) a 71 cm × 71 cm PVDF sheet. **Figure 2** illustrates the new configuration and a representative hydrophone record corresponding to the location of the scatterer. The extension of the sheet width to 71 cm delays the arrival of the edge wave to $\Delta t \approx 0.2$ ms after the initial pulse such that the low frequency roll-off of the spectrum begins at $1/(2\Delta t) \approx 2.5$ kHz. The high-frequency spectral and temporal properties of the radiated impulse (visible on the left side of the lower part of **Fig. 2**) were modeled by application of our previous result[J9] showing the following proportionality holds for the spectral region of interest:

$$p(t - t_o) = Ki(t), \quad i(t) = \text{current into sheet}, \tag{1}$$

p = pressure amplitude of plane wave (does not include edge wave)

t_o = propagation time to observation point

K = constant determined by piezoelectric properties

To approximate i(t) for a step voltage source, the lumped electrical parameter circuit model shown in **Figure 3(a)** was introduced with the result that the current is:

$$i(t) = \theta(t) i_o e^{-t/RC}, \quad i_o = V_o/R \tag{2a,b}$$

where θ is a unit step function and C denotes the sheet capacitance. Ordinarily the added resistance R_A may be neglected but to test the model various resistances R_A were inserted and the resulting increase in the exponential decay time of the radiated pressure impulse was observed. The spectrum of the current i(t) and acoustic pressure $p(t - t_o)$ was computed. Normalized such that the spectral amplitude $S(\omega)$ becomes unity at zero frequency, the magnitude is

$$|S(\omega)| = \left[(\omega RC)^2 + 1 \right]^{-1/2}. \tag{3}$$

Figure 3(b) shows an example of how this magnitude (the smooth curve) fits the spectrum of the hydrophone signal for Kaduchak's 44 cm × 44 cm sheet source. The observed peak (near 300 kHz) and subsequent roll-off (above 350 kHz) are a consequence of the fundamental resonance of the hydrophone. In the model, the effective sheet electrical

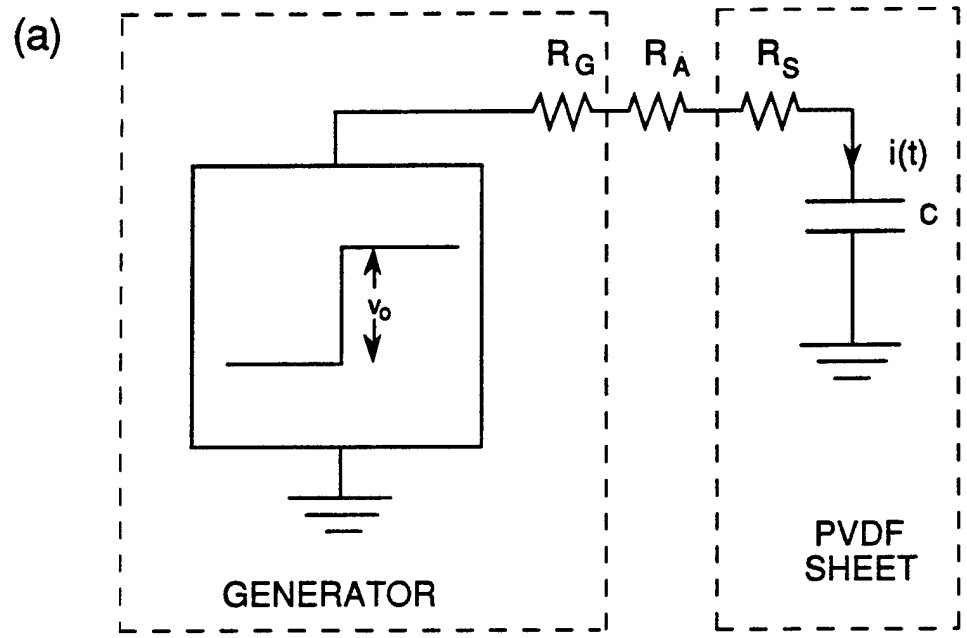

$R = (R_G + R_S) + R_A$

R_G = generator source resistance < 0.2 Ω for FET source

R_S = effective sheet resistance

R_A = added resistance (usually zero)

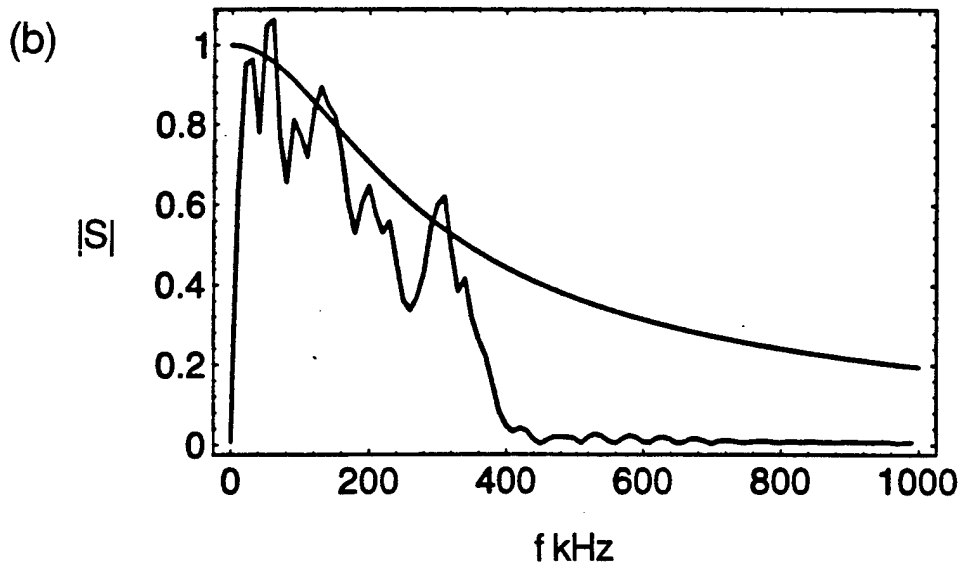

Figure 3(a) Transducer model and (b) spectrum.

resistance R_S was adjusted to fit the spectrum giving $R_S \approx R = 2$ ohms. The unusually broad spectral properties of the source could be extended to even higher frequencies with the use of suitable hydrophone. Acquisition of target spectral data in the 10 kHz to 400 kHz range was previously described.[J9]

A sheet source was also tested with tone burst excitation for target scattering experiments. It was found to be useful for a frequency range where tone burst sources are not generally available that are free from spurious ring-down tails.

2. Observations of the bipolar specular reflection and the dependence on the mass-per-area of a shell.

One prominent feature of the impulse response of shells that we previously reported[T3] and analyzed[J9] is the bipolar specular feature. A brief summary of the analytical model is needed to facilitate a description of the experiments. The model is appropriate to the early-time reflection of a pressure impulse by an empty spherical or cylindrical shell at normal incidence with other limitations noted below. Let $T = tc/a$ where a is the local shell radius of curvature and c is the sound speed in water. The early time pressure impulse response is proportional to the Fourier transform of the reflection coefficient R(x) where $x = ka = \omega a/c$ is the scaled frequency and R is approximated as described in Sec. A7. The specularly reflected farfield pressure becomes proportional to

$$P(T) = \frac{1}{2\pi}\int_{-\infty}^{\infty} R(x)\exp(-ixT)dx = \delta(T) - 2x_N e^{-t/t_N}\theta(T)$$

$$x_N = \rho a/\rho_E h = \text{null frequency}, \quad \rho_E h = \text{mass/area of the shell of thickness h}, \qquad (4)$$

$$t_N = \rho_E h/\rho c = \text{decay time of negative feature},$$

where δ is a delta function and θ is a unit-step function. The initially positive delta function specular reflection is followed by an exponentially decaying negative feature resulting from the finite inertia of the shell. Experimental and computational evidence of this result was discussed previously by us for spherical shells[J9,T3] and an additional computational test of the magnitude of the negative feature is given in Kaduchak's dissertation.[T1] While our original derivation was based on the aforementioned Fourier transform, Marston has recovered Eq. (4) by differentiation of an approximate Laplace transform analysis of the pressure step-response of a spherical membrane [Milenkovic and Raynor, J. Acoust. Soc. Am. *39*, 556-563 (1966)]. Analytical or experimental descriptions of the bipolar specular

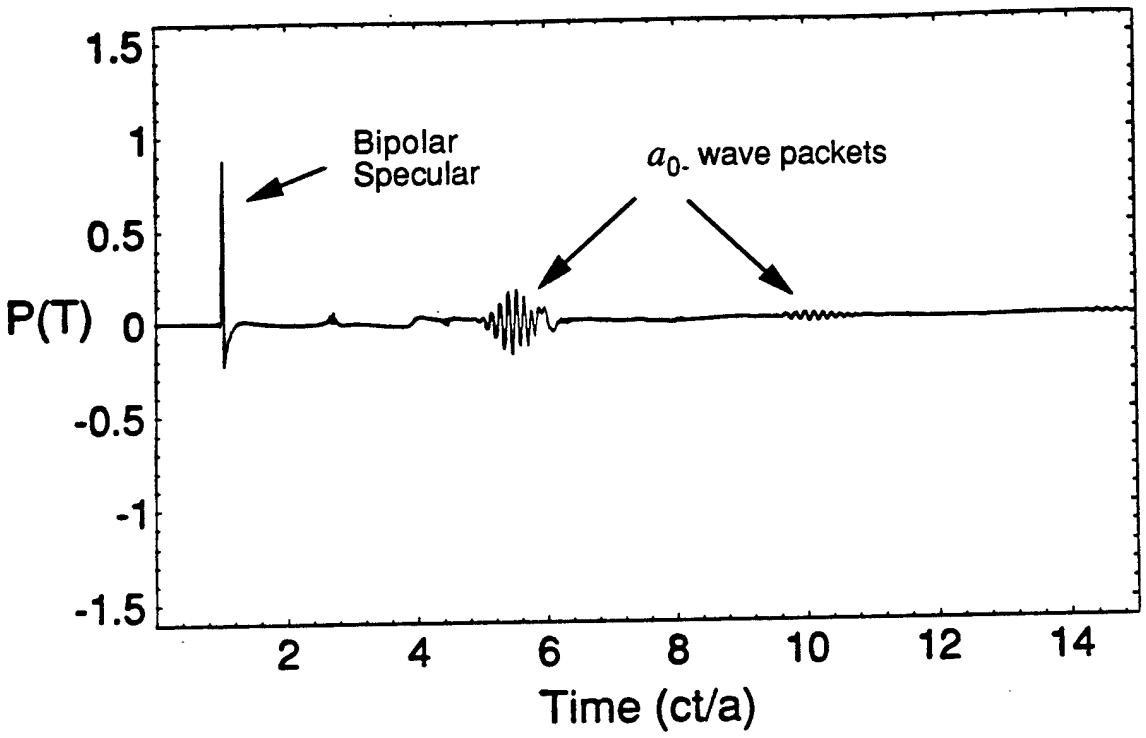

Figure 4

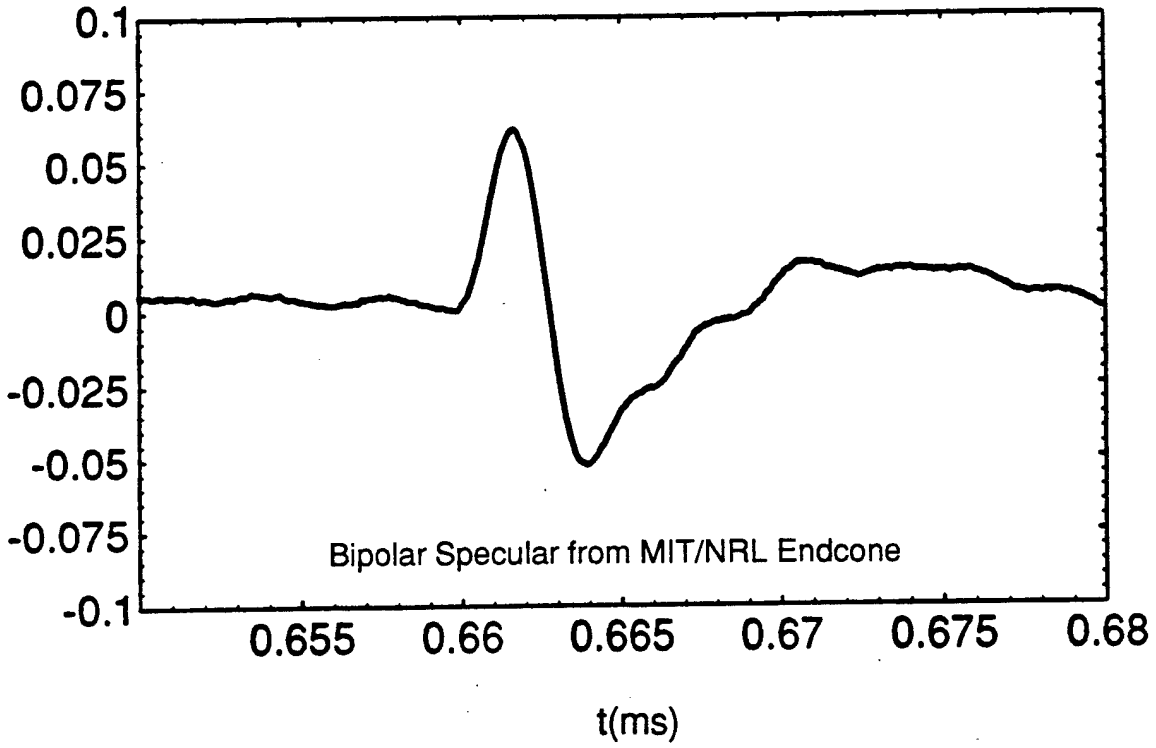

Figure 5

feature appear to have been lacking prior to our study[J9,T3] since to resolve this feature the width of the incidence impulse needs to be somewhat less than t_N. We also studied the negative portion of the bipolar feature in other new calculations and experiments which serve to clarify the assumptions and general nature of this feature. The results are summarized as follows:

(a) Computational study showing the negative part of the bipolar feature is only weakly affected by placing water on the interior of the shell: The calculated impulse responses were compared by evaluating the FFT of the form function filtered [as in Kaduchak and Marston, J. Acoust. Soc. Am. *93*, 2700-6 (1993)] to smooth the transient steps across the width of the shell that are usually not resolved in the experiment. The impulse responses were evaluated and compared for a 2.5% thick spherical shell as well as for an identical shell filled with water and one filled with water having an artificially large attenuation of sound.[T1] (The attenuation was introduced to isolate certain features of the late-time response.) The result of the third calculation is shown in **Figure 4**. The bipolar feature begins at $ct/a = 1$ and the relaxation of the negative feature is clearly visible. The relaxation time t_N appears to be only slightly smaller than in the corresponding feature calculated for an empty shell.

(b) Observations with the empty endcap of an MIT/NRL model shell: A ribbed nickel alloy shell having spherical endcaps (connected to the shell by short conical sections) has been studied with bandlimited transients at NRL [see Bondaryk and Schmidt, J. Acoust. Soc. Am. *97*, 1067-77 (1995)}. Since the spectrum of the incident transient used in the NRL experiments typically rolls-off above 50 kHz, the time resolution is not sufficient to isolate the details of the bipolar feature predicted by us. To facilitate our observations an extra endcone was borrowed from I. Dyer (MIT) and mounted in the WSU tank with the spherical end close to the sheet source. An example of one of the resulting time records is shown in **Figure 5**. The relaxation of the negative feature is clearly observed with the relaxation time being close to the predicted value from Eq. (4) of $t_N \approx 4.3$ μs where the thickness of the Ni alloy shell is 0.73 mm.

(c) Observed scattering by an empty thick cylindrical shell: The bipolar feature was also observed for scattering of an impulse by a thick cylindrical shell with the arrangement shown in **Figure 6**. Only the broadside results will be discussed here. The cylinder was filled with air and sealed with small rubber plugs on the ends. **Figure 7** compares calculated and observed features of the broadside response. The calculation is

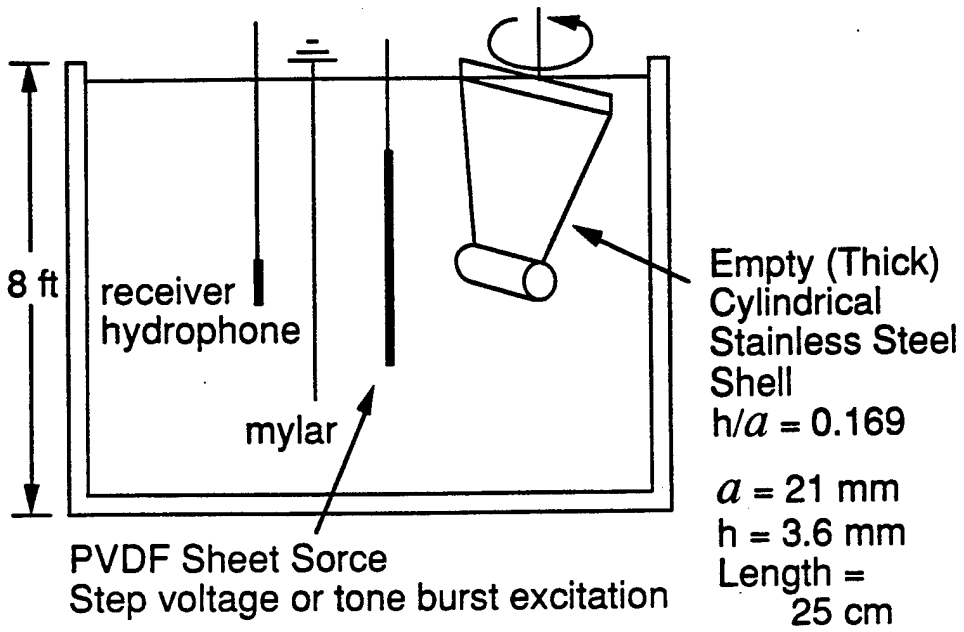

Figure 6 (above)

Figure 7 (below)

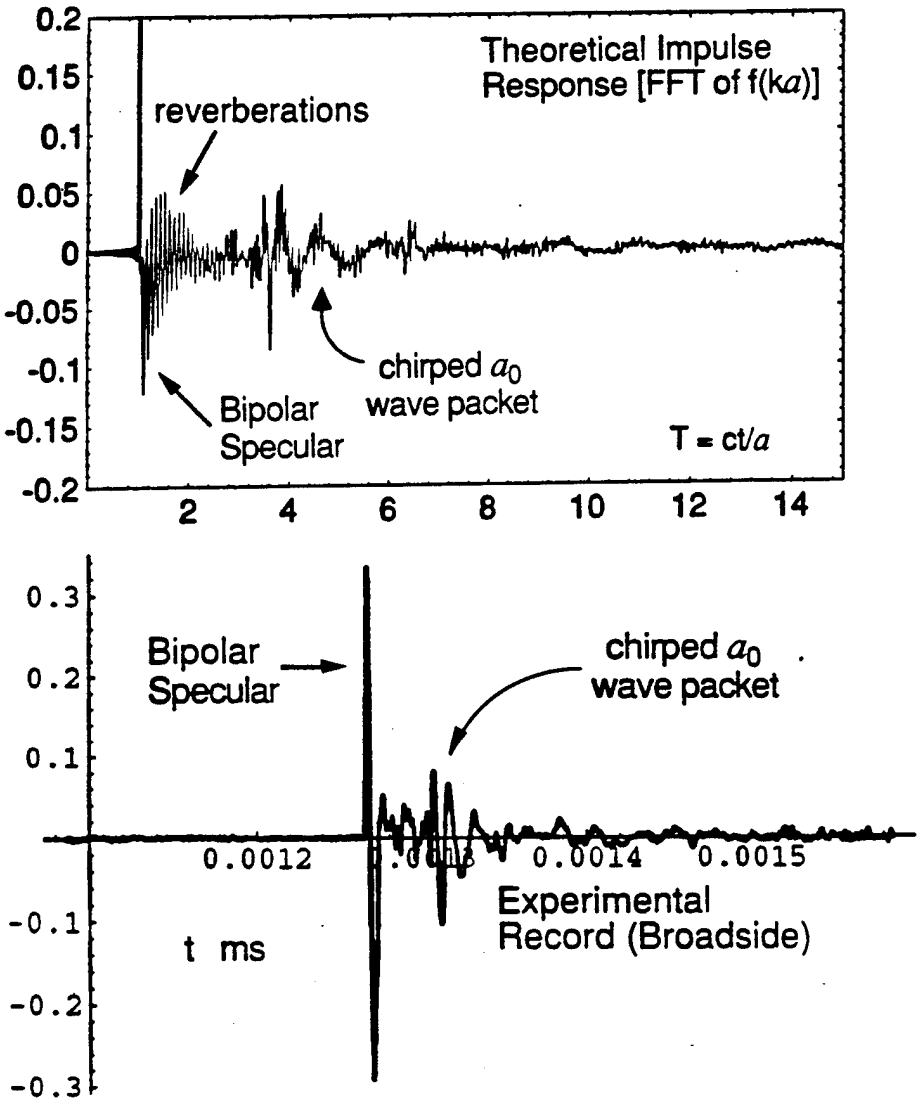

the FFT of the form function of an infinitely long cylindrical shell. The shell is thick having $h/a = 0.169$ so the reverberations of waves traveling across the thickness are more greatly spaced than in our other calculations. These reverberations are superposed on the negative feature of the calculated bipolar response. While the negative part of the bipolar feature is clearly visible in the experimental record, the reverberations are not resolved by the hydrophone.

3. Guided-wave features of the pressure impulse response of shells and mode beating: Observations and theory.

Observations and calculations in the previous Annual Report[T3] and our publication[J9] were extended to new situations summarized below. We also investigated guided-wave theory for a class of spheroidal shells in Appendix B of Ref. J7.

(a) Guided-wave contributions to scattering by a thick cylindrical shell: The configuration is shown in **Figure 6** with the shell air-filled and sealed by rubber as previously noted. Only the broadside results shown in **Figure 7** will be discussed here. After the bipolar specular feature has relaxed, the next prominent low frequency feature visible on both the theoretical and experimental records is a wavepacket chirped from high-to-low frequency. To identify the cause of this new feature in the thick-shell impulse response, the dispersion relations were calculated for guided waves using the full elasticity theory and Watson methodology as described by us in previous publications.[J7] The dispersion relations for the ka region of interest are shown in **Figure 8** where c_l is the phase velocity of the lth guided wave and β_l as the radiation damping. The analysis shows that the chirped wavepacket is a consequence of a guided wave labeled a_0 which shows a transaction from subsonic to supersonic behavior. Calculation of the group velocity of this wave shows that the high-frequency components of the wavepackets are backscattered earlier than the lower-frequency components as manifested by the chirped signal in **Fig. 7**.

(b) Beating of the low-frequency modes of thin shells excited by a pressure impulse: In our previous observation of the impulse response of a thin spherical shell[J9,T3] the millisecond time window for the experiment would only allow the first few cycles of the lowest frequency modes to be observed. To gain an understanding of the late-time behavior of these modes Scot Morse used smaller thin stainless steel spherical shells than previously studied. The small size pushed the coincidence frequency (and some of the other elastic features) above the frequency response of the hydrophone. **Figure 9** shows calculated (a) and measured (b) band-limited impulse responses for an empty stainless steel spherical shell having a diameter of 1.9 cm and a thickness to radius

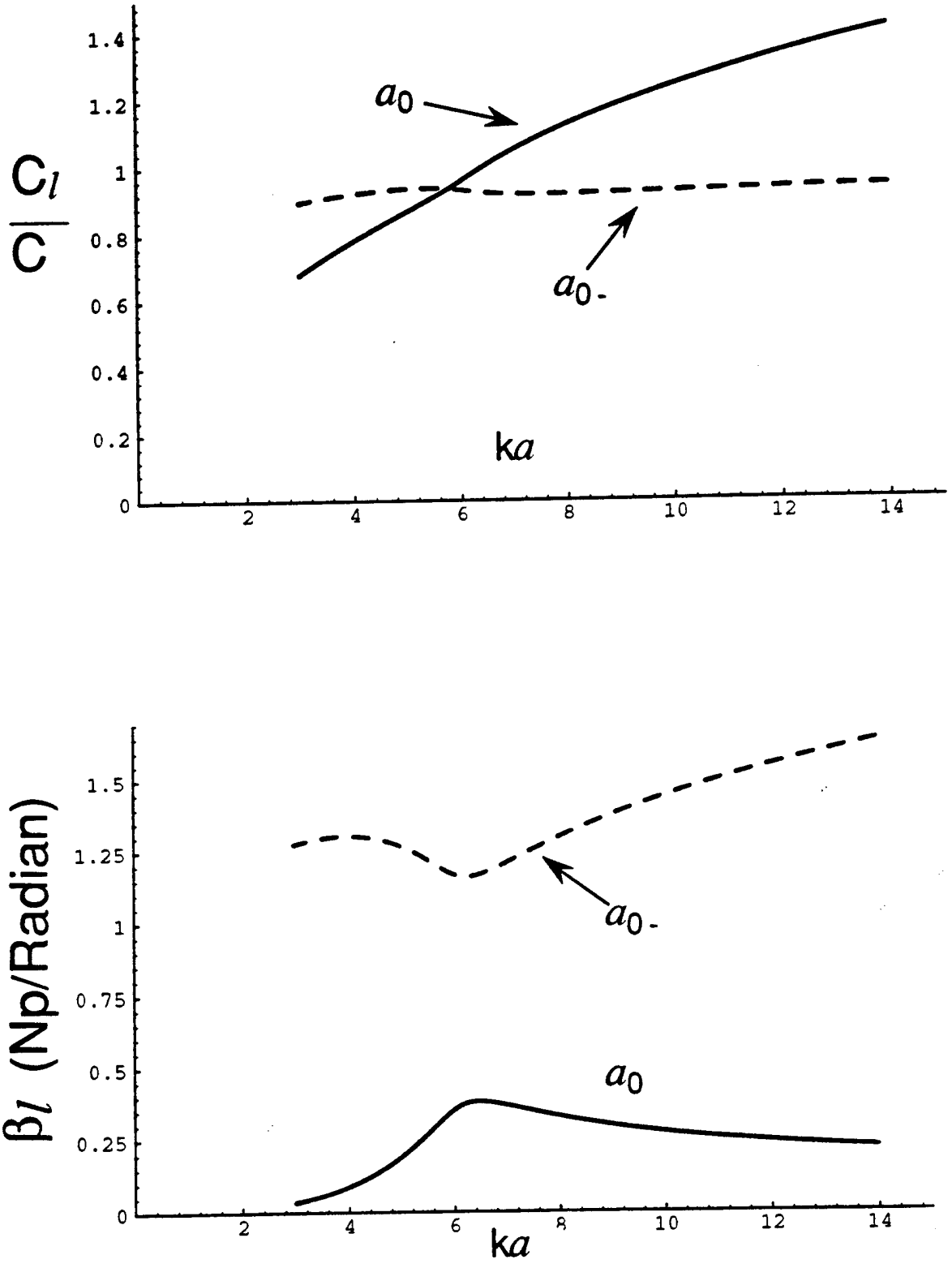

Figure 8. Calculated dispersion and damping in the coincidence region of the thick cylindrical shell used in Figs. 6 and 7. The curves have important qualitative differences with thin shell results and they explain our measurements.

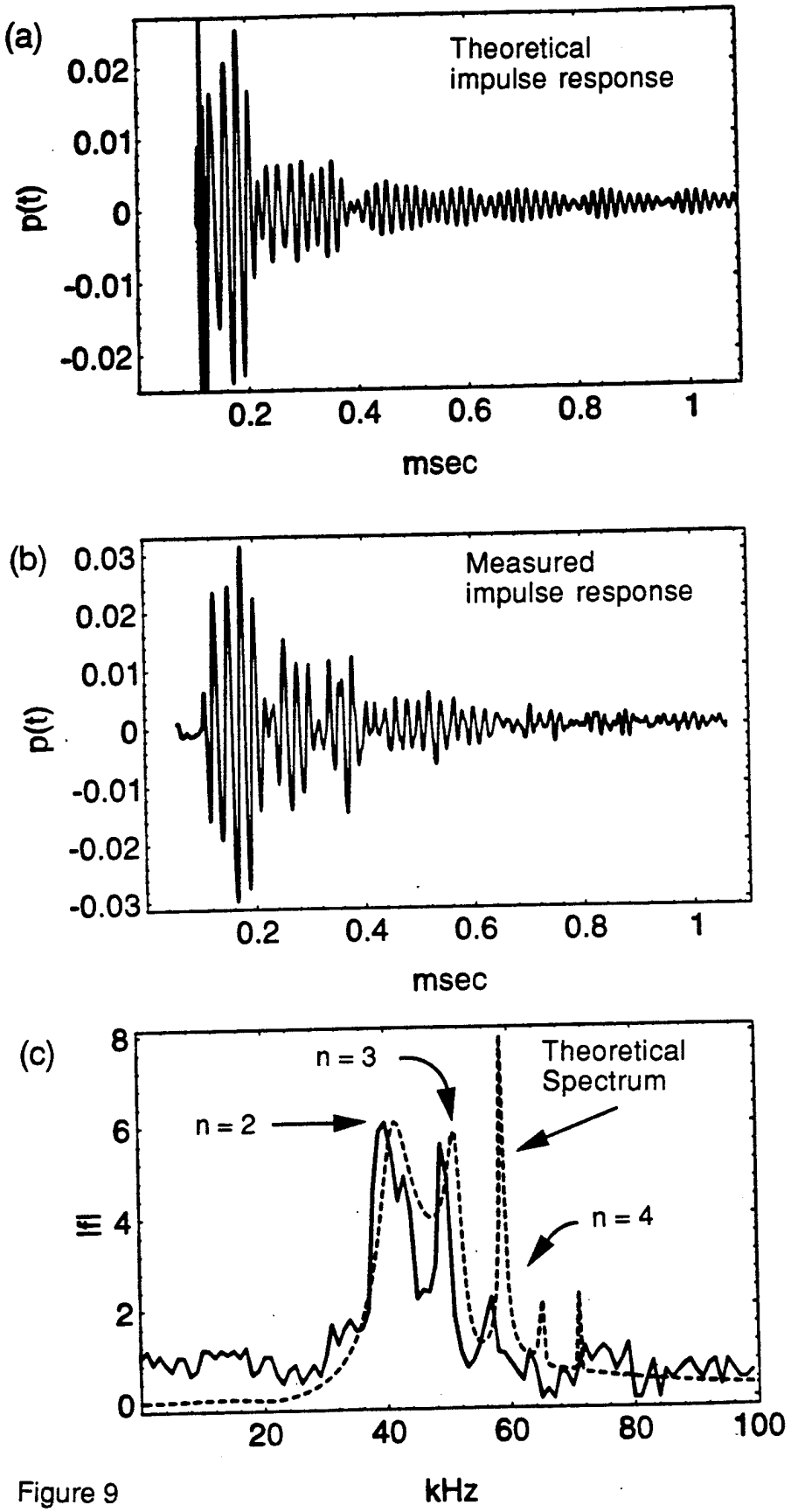
(a)
Theoretical
impulse response
0.02
0.01
0
-0.01
-0.02
p(t)
0.2
0.4
0.6
0.8
1
msec
(b)
Measured
impulse response
0.03
0.02
0.01
0
-0.01
-0.02
-0.03
p(t)
0.2
0.4
0.6
0.8
1
msec
(c)
n = 3
Theoretical
Spectrum
n = 2
n = 4
8
6
4
2
0
|fi|
20
40
60
80
100
kHz

Figure 9

ratio of 0.035. In (c) the calculated (dashed) and measured (solid curve) spectra are shown. The measured spectrum is the FFT of the record in (b). It is scaled in amplitude such that the peak near 40 kHz corresponds to the predicted amplitude calculated for an infinite duration record. The first three predicted peaks correspond to the n = 2, 3, and 4 partial waves and are associated with the lowest flexural modes of the shell (see e.g. Appendix D of Ref. J9). These modes are evident in the measured spectrum. The beating between these modes produces the envelopes of the calculated and measured signatures in **Figs. 9** (a) and (b) and these envelopes are similar in appearance. For a different shell having water on the inside observations were obtained where only two modes were excited and the beating pattern is much simpler.

(c) Coincidence frequency wavepacket in the impulse response of a water-filled thin shell: A prominent high-frequency feature of the thin shell impulse response is the coincidence frequency wavepacket associated with the a_0- wave.[J9] Kaduchak [T1] carried out a computational study to determined whether the a_0- wavepacket would be completely quenched if water is on the inside of the shell. The method was to evaluate the FFT of the form function of a water filled shell. As explained in Section 2(a) the calculations were also used to investigate the bipolar specular feature and were done with a shell having $h/a = 0.025$. In the absence of attenuation within the water interior, the wavepacket is present but arrives at the same time as other strong scattering contributions attributable to waves transmitted through the walls of the shell. By artificially adding attenuation to the inner water, these waves can be quenched and the first three circumnavigations of the a_0- wavepackets are clearly evident in **Figure 4.**

4. Retro-reflective backscattering of sound due to Rayleigh waves on a solid rectangular parallelepiped.

Consider a solid object cut with square corners which may have a random orientation relative to the direction of incident sound from a high-frequency sonar. The question of interest is to identify the most likely mechanism for producing a strongly backscattered signal. Research carried out by K. Gipson has confirmed the existence of a mechanism that is more likely to occur than simple specular reflection back towards the source.[M10] (The specular mechanism requires that two of the Euler angles of the scatterer lie in a narrow range while the mechanism studied here puts narrow limits on only one of the Euler angles.) The novel mechanism is illustrated in **Fig. 10**: a Rayleigh wave is launched on the stainless-steel block in water such that after reflection from two edges the radiated wavefront is directed back towards the source. It is necessary only that the angle

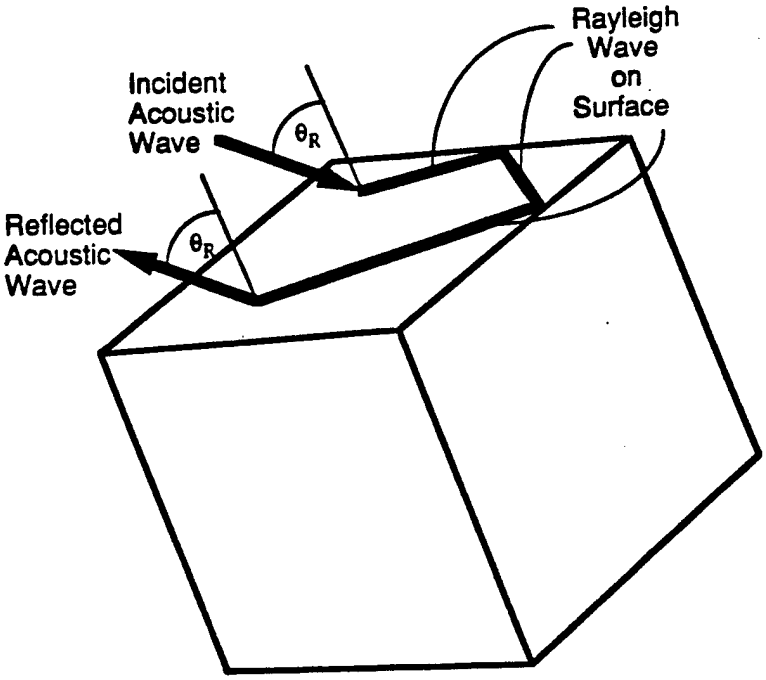

Figure 10. Ray diagram of backscattering enhancement for an elastic solid with square corners.

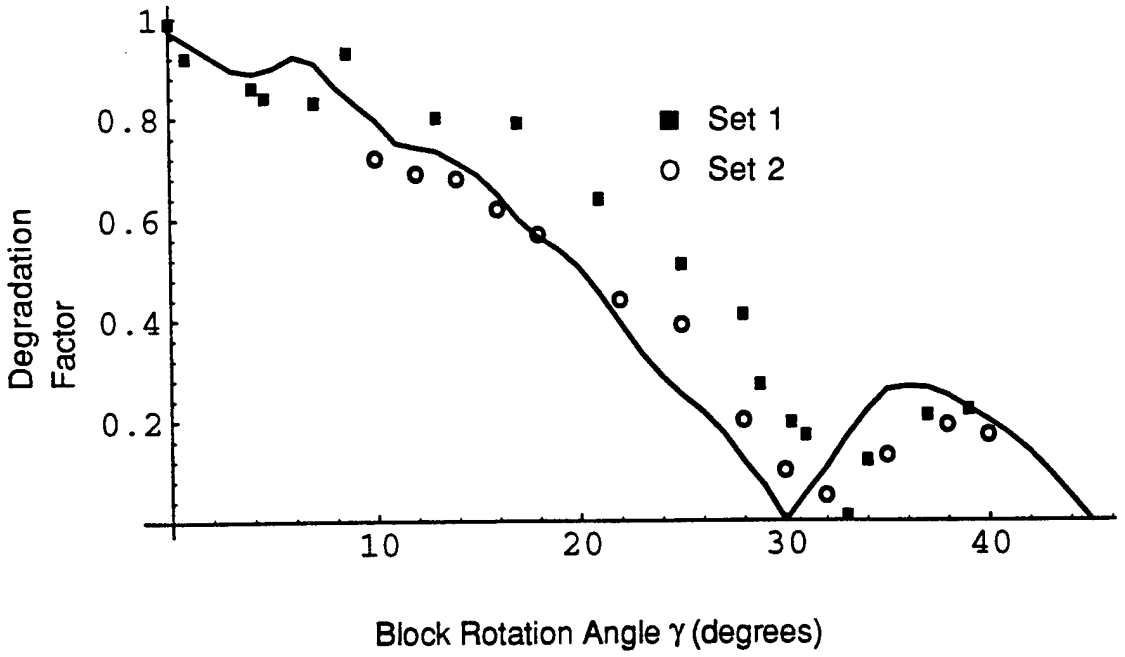

Figure 11. Plot of normalized backscattering at 1.5 MHz as a function of the rotation angle of the steel block. The angle of incidence θ is fixed at the Rayleigh angle θ_R.

of incidence θ lie within about a degree of the Rayleigh angle θ_R of the elastic material. This was demonstrated in last year's report[T3] along with results of an approximation based on the convolution formulation[J10] for leaky wave scattering contributions, Eq. (5). During the current period Gipson extended the measurements by rotating the block relative to the source at fixed angle of incidence $\theta = \theta_R$. (The experiment used a rotary stage and laser alignment system.) The degradation of the backscattering with rotation angle γ is given by the product $D(\gamma) = B(\gamma)\, F(\gamma)$ where $F(\gamma) = (1 - \tan^2\gamma)/(1 + \tan^2\gamma)$ is a geometric factor and $B(\gamma)$ is a product of Rayleigh wave reflection coefficients off of the block corners normalized to the value at $\gamma = 0$. The factor B may be approximated by making use of computational results of Gautesen [Wave Motion *8*, 27 (1986)] for oblique Rayleigh wave reflection at an elastic quarter space in a vacuum. A comparison of the measurements (points) with the approximate theory (curve) is shown in **Figure 11**. The important result is that the slow decrease of $D(\gamma)$ with increasing γ confirms the backscattering depends only weakly on the Euler angle γ. Some of the discrepancy may result from Poisson's ratio of the steel block differing slightly from the value of 1/3 used in Gautesen's computation.

A connection between this work and experiments on plates carried out at ARL (University of Texas) during Marston visit (Spring 1993) is noted in last year's report.[T3]

5. Torsional and edge wave excitation on a plate with an EMAT.

In our previous work Matula measured the acoustic wavefield in water and the transition radiation that occurs when a subsonic flexural wavepacket on the plate first crosses the free surfaces of the water. This work is summarized in the abstract of his recent publication[J8] from the *Journal of the Acoustical Society of America* reproduced here in **Figure 12**. In those experiments a specific type of Lamb wave corresponding to a flexural wave was excited with an EMAT (electromagnetic acoustic transducer). The plate was 16 feet in length and was hung with its lower half in the water. To facilitate possible future investigations of the acoustic wavefield for more complicated excitations on the plate Dave Ermer[J1] modified the EMAT such that the induced electrical currents in the plate would be asymmetric across the width (the wide-dimension) of the plate. Since the plate is in a uniform magnetic field, this resulted in asymmetric Lorentz stresses which were used to excite wavepackets of torsional and edge wave spatial modes on plate. (This new EMAT configuration may be contrasted to the configuration shown in Fig. 3 of Matula's publication[J8] where the stresses are uniform across the wide dimension.) Ermer's experiments were done with the plate entirely in air but, as in Matula's experiments, a tone burst excitation was used of sufficient duration to simulate steady-state excitation. The spatial distribution of the excited wavepacket across the wide dimension of the plate was

Energy branching of a subsonic flexural wave on a plate at an air–water interface. I. Observation of the wave field near the interface and near the plate

Thomas J. Matula[a)] and Philip L. Marston
Department of Physics, Washington State University, Pullman, Washington 99164-2814

(Received 27 April 1994; revised 25 August 1994; accepted 25 October 1994)

The radiation of subsonic flexural plate waves due to a discontinuity in fluid loading is experimentally investigated. A tone burst of flexural waves propagates down a plate, the lower section of which is submerged in water. Measurements indicate that there occurs a branching of energy as the flexural wave passes through the air–water interface, with little reflected energy. A portion of the transmitted energy continues along the plate as a subsonic flexural wave with an associated acoustic evanescent wave. A second acoustic wave (which is termed transition radiation) originates at or near where the plate crosses the interface, and propagates in water to the far field. In the near field of the interface there exists an interference between the two acoustic waves in water that results in a series of pressure nulls. The pressure nulls are associated with a π phase change in the wave field and are indicators of wavefront dislocations. A numerical computation of the wave field in an unbounded fluid due to a line-moment excitation of a plate has similar features as the null pattern observed but differs in certain details.

[a)]Present address: Applied Physics Laboratory, University of Washington, 1013 NE 40th St., Seattle, WA 98105.

Figure 12

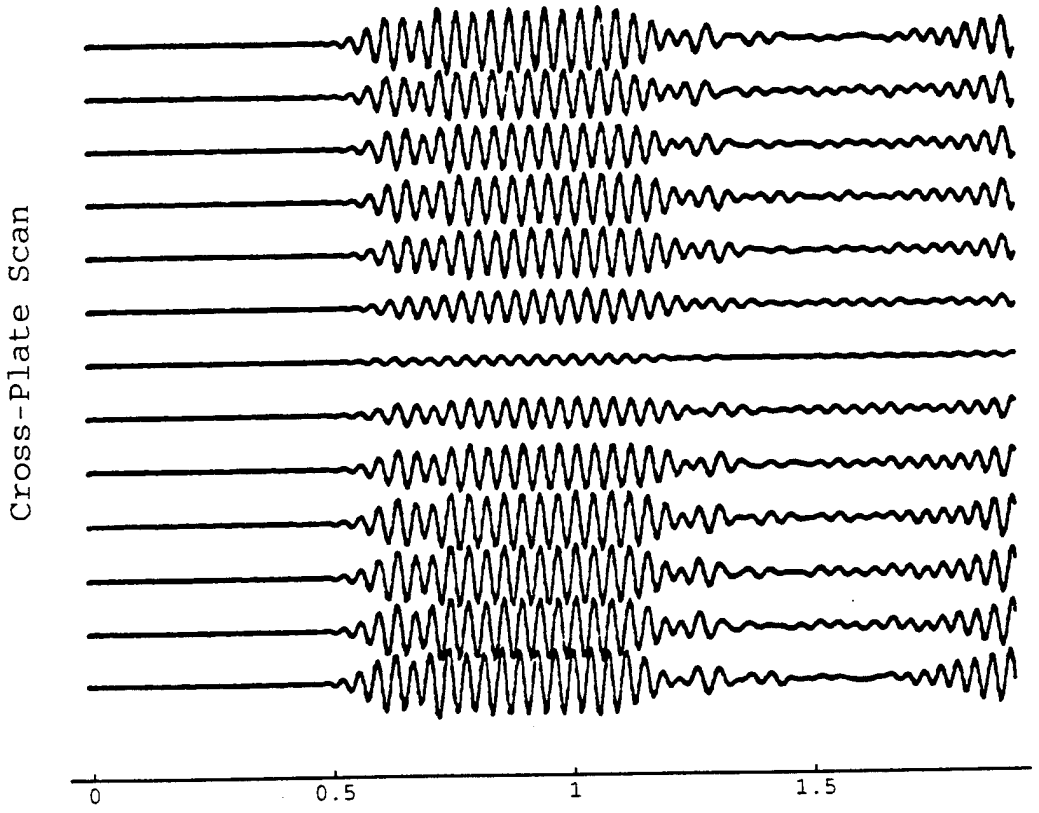

Figure 13

determined by mechanically scanning a small microphone at a fixed distance from the plate. The microphone was also scanned down the plate to determined the phase and group velocities of the wave. **Figure 13** shows an example of the microphone output for a cross-plate scan when a 27 kHz torsional packet is excited on the plate. As expected the signal is antisymmetric across the width, being weak near the centerline. The measured phase velocity of 876 m/s is close to an approximate predicted value of 899 m/s and, as expected, the measured group velocity of 1600 m/s is much greater.

6. Convolution formulation of leaky wave contributions to scattering by cylinders of variable curvature or with truncations: Examples for partially-coated or S-shaped surfaces and the merging of launching or detachment points.

To facilitate the approximation of leaky wave contributions to high-frequency scattering by complex objects, a convolution formulation was developed by Marston[J4,J10] that is not based on the assumptions of thin shell theory. The abstract of the principal publication[J10] is reproduced in **Figure 14(a)**. **Figures 14(b)** and **(c)** illustrate applications to partially coated or variable curvature surfaces considered there. The formulation approximates the amplitude of the radiated leaky wave contribution at a surface point parameterized by an arc length s along the surface. It is related to the incident wave amplitude $p_i(s')$ at s' by the following convolution with the one-sided spatial response function h

$$p_l(s) \approx \int_{-\infty}^{s} p_i(s')h(s - s';s,s')ds' \quad , \tag{5}$$

where the one-sided line response h depends not only on (s - s') but also weakly on s and s' through any dependence on curvature of the local leaky wave properties. These properties are the real component k_l and imaginary component α of the wavenumber for the lth leaky wave. With fluid loading on only one side of the surface[J10]

$$h(s - s';s,s') \approx -2\left[\alpha(s)\alpha(s')\right]^{1/2} H(s - s') \exp\left[i\varphi_{bl} + i\int_{s'}^{s} (k_l + i\alpha)ds' \right] \quad , \tag{6}$$

where H is a unit-step function and φ_{bl} is the phase of the plane surface reflection coefficient of plane surface reflection at the leaky-wave angle of incidence $\theta_l = \sin^{-1}(c/c_l)$.

Leaky waves on weakly curved scatterers. II. Convolution formulation for two-dimensional high-frequency scattering

Philip L. Marston[a)]
Department of Physics, Washington State University, Pullman, Washington 99164-2814 and Advanced Sonar Division, Applied Research Laboratories, University of Texas at Austin, Austin, Texas 78713-8029

(Received 16 April 1994; accepted for publication 24 August 1994)

(a)

A simple high-frequency approximation is developed for leaky wave contributions to two-dimensional scattering by curved elastic surfaces. Following Bertoni and Tamir [Appl. Phys. **2**, 157–172 (1973)] the method relies on general features of the Laurent expansion of the plane surface reflection coefficient $R(k_x)$ about the leaky wave pole of interest at the complex surface wave number $k_x = k_l + i\alpha$. The formulation uses the real part k_l and radiation damping rate α for leaky waves on the curved elastic surface of interest rather than an analysis of the response of any specific class of structures such as thin shells. The high frequency limit of the complex coupling coefficient G_l [see, e.g., P. L. Marston, J. Acoust. Soc. Am. **83**, 25–37 (1988)] is recovered for right circular cylinders and the physical origin of the $\pi/4$ phase shift is discussed. An $O(kh)^{-1}$ phase correction important for empty thin shells of thickness h is obtained in agreement with results from other approaches. The importance of the Fresnel width of the coupling region is illustrated by consideration of a cylinder with an ideal coating having an abrupt edge. The leaky wave contribution becomes proportional to a Fresnel integral having a complex argument. The integral manifests the degree to which launching of a leaky wave can be considered to be a local process. The product of α and the Fresnel width is an important parameter. The detachment of the ray to the far field is taken to be separated from its launching by more than the Fresnel width. Leaky wave contributions to scattering by surfaces of variable curvature are approximated and applications for ultrasonic beams are noted.

[a)]Present and permanent address: Washington State University.

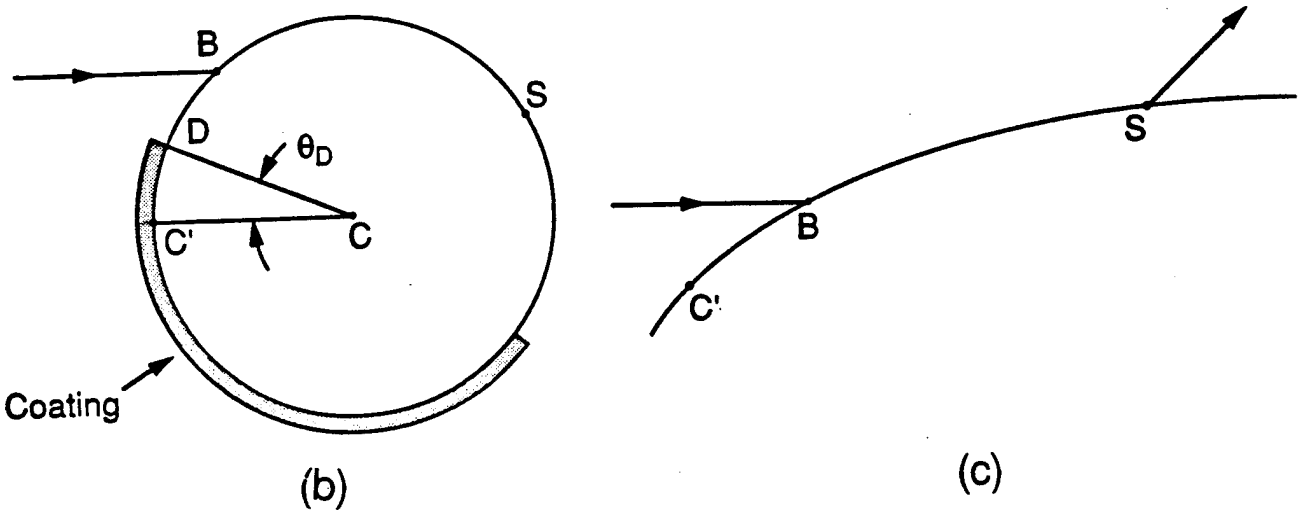

Figure 14

The phase of the integrand of Eq. (5) depends not only on h but also on the shape of the surface and the direction of the incident wave through $p_i(s')$. A stationary phase for some value of s' corresponds to the coupling of a leaky wave onto the surface within a Fresnel width of at that point.[J4] The outgoing amplitude is propagated to the observer. For the special case of a circular cylinder previous results for the coupling coefficient G_l are obtained at high frequencies. As the frequency is lowered, wave kinematic corrections to $\arg(G_l)$ may become significant as discussed e.g. in Marston's forthcoming *Wave Motion* paper[J12] discussed in last year's *Report*.[T3] The present formulation illustrates the effects of truncations (such as a partial coating shown in Fig. 14(b)) and variable curvature (Fig. 14(c)).

Surfaces of variable curvature may introduce some important complications that were examined by Marston.[M1] In the usual case there is only one stationary phase point corresponding to the launching of a leaky wave by a ray through point B in Fig. 14(c). There is also (for a given surface region) only one stationary phase point in the propagation integral to the observer, corresponding to the detachment point through S in Fig. 14(c). For some surface shapes, such as a tilted "S" shaped surface there may be two closely spaced launching points or two closely spaced detachment points. The launching points, for example may merge and disappear with variations in the direction of the incident wave. Marston's analysis for that situation[M1] predicts a $k^{1/6}$ amplitude enhancement factor for the simplest case of two merged launching or detachment points as well as an Airy function factor for which argument vanishes when the stationary points merge. Orientation of the surface such that there are no stationary phase points of the integral in Eq. (5) correspond to the shadow side of the Airy function. In that case the launching of the leaky wave is attributed to a "complex ray."

7. Phase of the background contribution for scattering by shells.

In addition to various scattering contributions by guided waves and truncations considered for example in Sec. 6, an important contribution is the background contribution usually associated with specular reflection. That contribution causes the bipolar specular feature in the pressure impulse response discussed in Sec. 2. The phase of the coupling coefficient G_l is linked to the background in a way discussed by Marston.[M13] In the new research, various approaches to the background and phase were compared to gain a better understanding of their similarities and differences. For the purposes of this comparison attention will be restricted to specular reflection at normal incidence from an empty sphere or cylinder of outer radius *a* and thickness h. The background contribution $f^{(b)}$ to the relevant form function may be written

$$f^{(b)} = R \exp(-2ika) \ , \tag{7}$$

Where R may be interpreted as a complex effective reflection coefficient. A ray-theory approach to R is to approximate R using the lumped-mass inertia of a thin membrane having the same mass per area as the shell. That approach [see e.g. Norris and Rebinski, J. Acoust. Soc. Am. *95*, 1809-1829 (1994)] gives the unimodular

$$R(ka) = (x_N + ika)/(-x_N + ika) = e^{i\varphi} \ , \tag{8}$$

where x_N is the null frequency listed earlier in Eq. (4). That approximation gives the smooth negative specular feature described in Sec. 2 since it smoothes out the effects of reverberations across the thickness of the shell. Another approximation discussed by Kargl and Marston [J. Acoust. Soc. Am. *89*, 2545-58 (1991)] is to replace R by the unimodular reflection coefficient of a vacuum backed plate. In new research, Marston confirmed analytically and computationally that these approaches give similar values for the phase arg(R) at low frequencies but that the differences may be appreciable at high frequencies for a thick shell since Eq. (8) completely neglects the internal dynamics associated with a thickness resonance. A numerical comparison is shown in **Figure 15(a)** for the 16.2% thick stainless steel shell studied by Kargl and Marston. The dashed curve is from Eq. (8) with φ in radians while the solid curve is from the more realistic plate approximation.

Another approximation for $f^{(b)}$ has been proposed by Gaunaurd and Werby [J. Acoust. Soc. Am. *90*, 2536-50 (1991)] which also neglects the internal dynamics of the shell. That approximation which gives a simple form for the "background transition function" B(k*a*) introduced by Marston,[J12,M13] includes a wave-kinematic diffractive correction not present in Eq. (8). For the case of the sphere, we find

$$\arg(R) \approx \varphi - \tan^{-1}(3/2ka) \ , \tag{9}$$

where φ is defined as in Eq. (8) and the second term is the diffractive correction. A comparison is shown in **Figure 15(b)** that supports the use of Eq. (9). The short dashed curve shows φ for the example in **Fig. 15 (a)** while the curve with longer dashes is the right side of Eq. (9). The solid curve is from the Gaunaurd and Werby approximation. Equation (9) was derived by superposing inertial and diffractive corrections to the initial approximation of the form function. Comparisons were also plotted for thin shells.

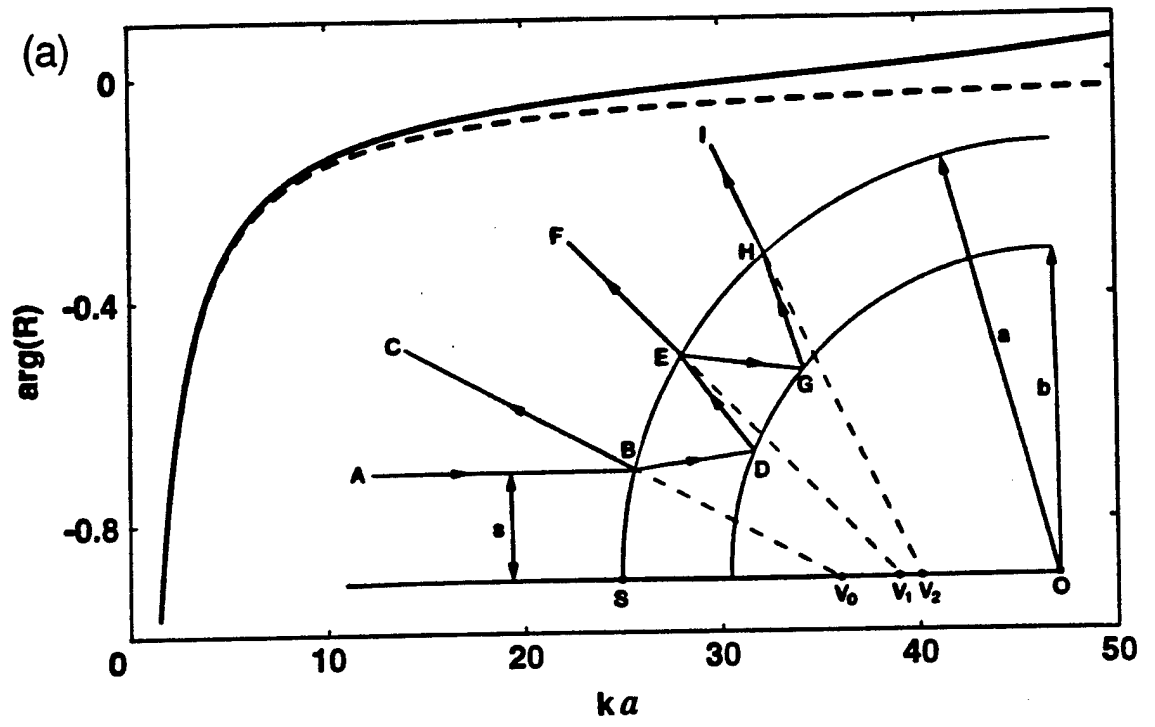
(a)
0
-0.4
-0.8
arg(R)
0
10
20
30
40
50
ka
I
F
H
C
E
G
a
b
B
A
D
s
S
V0
V1 V2
O

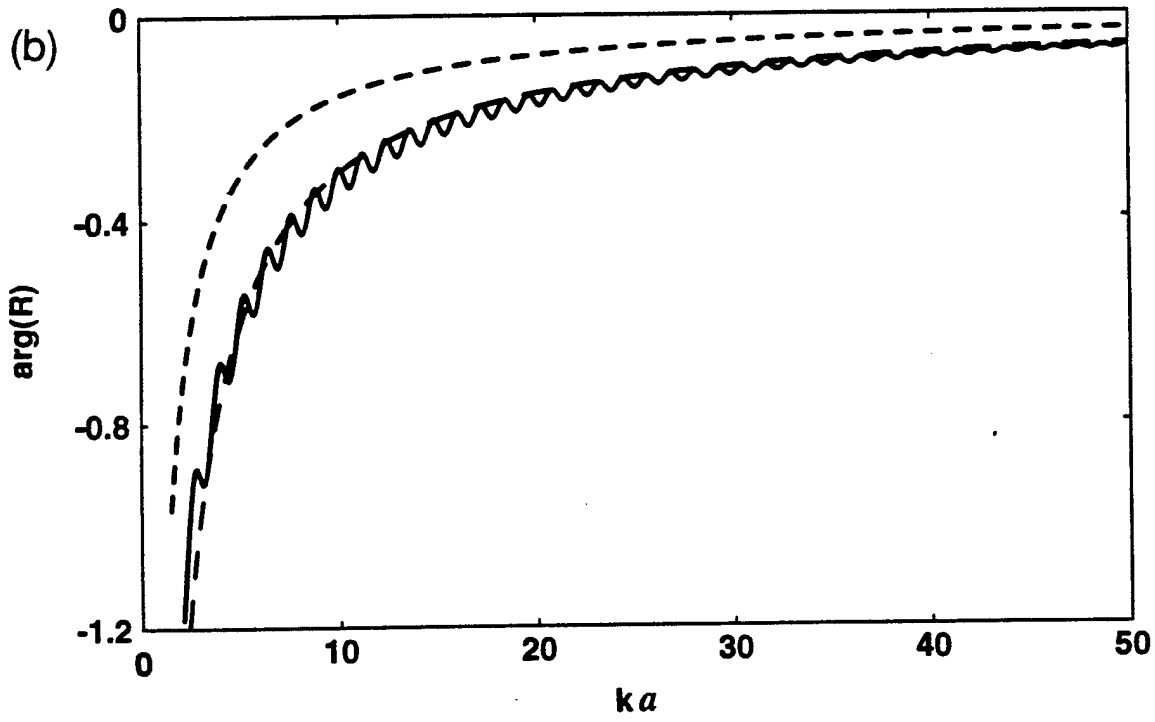
(b)
0
-0.4
-0.8
-1.2
arg(R)
0
10
20
30
40
50
ka

Figure 15

B. Wavefields of random caustics produced by reflection: Measurements of intensity moments and twinkling exponents.

When high-frequency sound is reflected from randomly corrugated surfaces, the reflected wavefield contains a region of large intensity fluctuations dominated by the presence of a network of random caustics. The effect of these caustics on the statistical properties of the wavefield is the subject of an investigation being carried out jointly with Dr. Kevin L. Williams of the Applied Physics Laboratory of the University of Washington. Experimental investigations were carried out at the water tank measurement facility at Washington State University by John Stroud. During the period of the present report Stroud completed his Ph.D. dissertation[T2] with the support of this grant and certain theoretical aspects of the research were published in the *Journal of the Acoustical Society of America*,[J5] The experimental results are summarized in Stroud's dissertation abstract reproduced in **Figure 16**. The intensity moments which characterize the wavefield fluctuations are defined as follows for the mth moment:

$$I_m = \langle I^m \rangle / \langle I \rangle^m \qquad (10)$$

where for the purposes of this discussion the "intensity" $I = |p|^2$ where p is the peak acoustic pressure of a reflected wavepacket having a known carrier frequency and normalized to account for a weak directionality of the wave incident on the surface. The angular brackets in Eq. (10) correspond to a spatial average over a specified region of the reflected wavefield. The nature of the fluctuations are evident in the scan of the reflected wavefield shown in **Figure 17** where the wavepacket incident on the surface was a 6 cycle pulse having a cosine squared enveloped with a 200 kHz carrier. (The axes are labeled in meters.) The brightest regions are the highest intensity regions of the reflected wavefield. These regions lie adjacent to the predicted locations of caustics shown as the curves in **Figure 17**. The measured wavefield shown is like the one synthesized by modifying our analysis[J5] to describe pulses. One important conclusion is that for the region shown the moments of the reflected wavefield do not correspond to those of a random phasor sum which gives a Rayleigh amplitude distribution and an exponential intensity distribution as is often assumed. Contrary to the behavior of an exponential distribution, which has $I_m = m!$, the I_m tend to increase with increasing wavenumber $k = \omega/c$. M. V. Berry [J. Phys. A. *10*, 2061-2081 (1977)] predicted (for situations like the one measured) the following high-frequency scaling behavior

Twinkling of underwater sound reflected by one realization from a Gaussian spectrum population of corrugated surfaces: Experiments and comparisons with a catastrophe theory approximation—John S. Stroud, Department of Physics, Washington State University, May 1995 (Ph.D.). Experimental and numerical investigations were carried out on sound in water reflected from a single realization of a population of Gaussian spectrum random rough surfaces. These investigations used ultrasound of various frequencies and pulse lengths to study a predicted scaling of intensity moments with frequency. The high-frequency scaling of the moments is a consequence of the caustics in the reflected wavefield. The resulting spatial fluctuations of the intensity are analogous to the scintillations or twinkling of light resulting from focusing and defocusing within the atmosphere. The surface properties (rms height and correlation length) are such that the Kirchhoff approximation may be used to calculate the reflected wavefield. Relevant conceptual tools and results from the branch of mathematics known as catastrophe theory are used to classify the types of contributions one expects as well as providing the scattered pressure amplitude for a given caustic. Catastrophe theory also provides the scaling properties of the intensity moments. The theoretical prediction that the second moment of intensity has a logarithmic dependence on the wave number is confirmed. The prediction that the third through the fifth moments depend upon the wave number in a manner as k^{ν_m} where m represents the mth moment and k is the wave number of the incident sound is also supported by the measurements. For Airy caustics, the theoretical values of the twinkling exponents ν_m are 1/3, 2/3, and 1 respectively. For the largest scan of the reflected wavefield recorded, the twinkling exponents were measured to be 0.30, 0.57, and 0.86. The dependence of the second moment on pulse length and distance was also measured. For long duration pulses and large distances from the surface, there is evidence of a transition towards a negative exponential intensity probability density function (PDF). A negative exponential PDF is characteristic of a Gaussian quadrature field associated with the interference of many contributors.

Figure 16 (above)

Figure 17 (below)

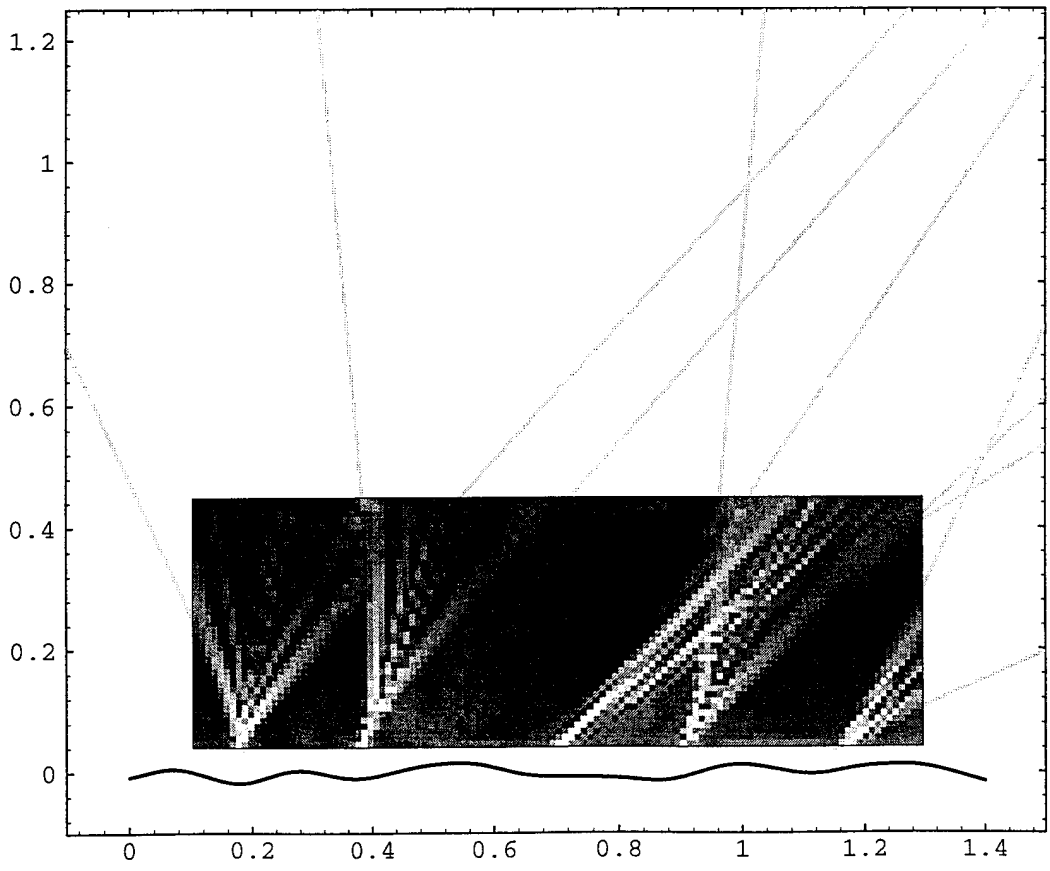

$$I_m = A_m k^{\nu_m}, \quad m > 2, \quad \nu_m = \text{twinkling exponent}. \tag{11}$$

This experiment is the first laboratory measurement of the ν_m for sound waves. The measured ν_m for m = 3, 4, and 5 lie close to the predicted values (see **Figure 16**). [For an introduction to random caustics see: P. L. Marston, Physical Acoustics *21*, 1-235 (1992) Sec. 3.14.] Other statistical measurements studied by Stroud include the variation of the second moment I_2 with distance from the surface and the duration of the incident pulse. The research has direct application to understanding the statistics of fluctuations in target strength resulting from high frequency sound reflected by smoothly curved surfaces.

C. Interaction of sound with sound mediated by a suspension of particles.

When a suspension of small particles is present in water, the interaction of sound with sound may be significantly enhanced by the following process: (i) a grating in the number density of suspended particles is induced by the spatially periodic radiation pressure of the standing wave formed by two of the incident waves and (ii) the reflection of an ultrasonic probe wave is greatly enhanced when the Bragg condition is met. This mechanism was originally demonstrated with ONR support in the Ph.D. dissertation of H. J. Simpson.[T3] During the period under review, the theory for the interaction was submitted and accepted for publication in the *Journal of the Acoustical Society of America*.[J11] Kwiatkowski made the following experimental and theoretical advances.[M14]

1. Collinear four-wave mixing mediated by a suspension.

The previous experimental work was limited to oblique Bragg reflection and therefore required meticulous alignment. In the new geometry the probe wave propagates along the same axis as the pump standing wave as shown in **Figure 18**. A PVDF sheet is placed at one end of the standing wave resonator which is the source of the probe wave as well as the receiver of the Bragg reflected signal. The pump frequency is typically 770 kHz while the probe wave is scanned in the range 1.5 to 4 MHz. Another innovation is that hollow glass microspheres are used for the suspension to facilitate varying the concentration over a wide range. Varying the duration of the probe tone burst has approximately the same effect as varying the number of layers in the grating since the number of layers illuminated by the incident sound is proportional to the duration. The theory indicates that the frequency width of the Bragg peak varies inversely with the duration of the probe burst. This prediction is confirmed by the comparison with theory

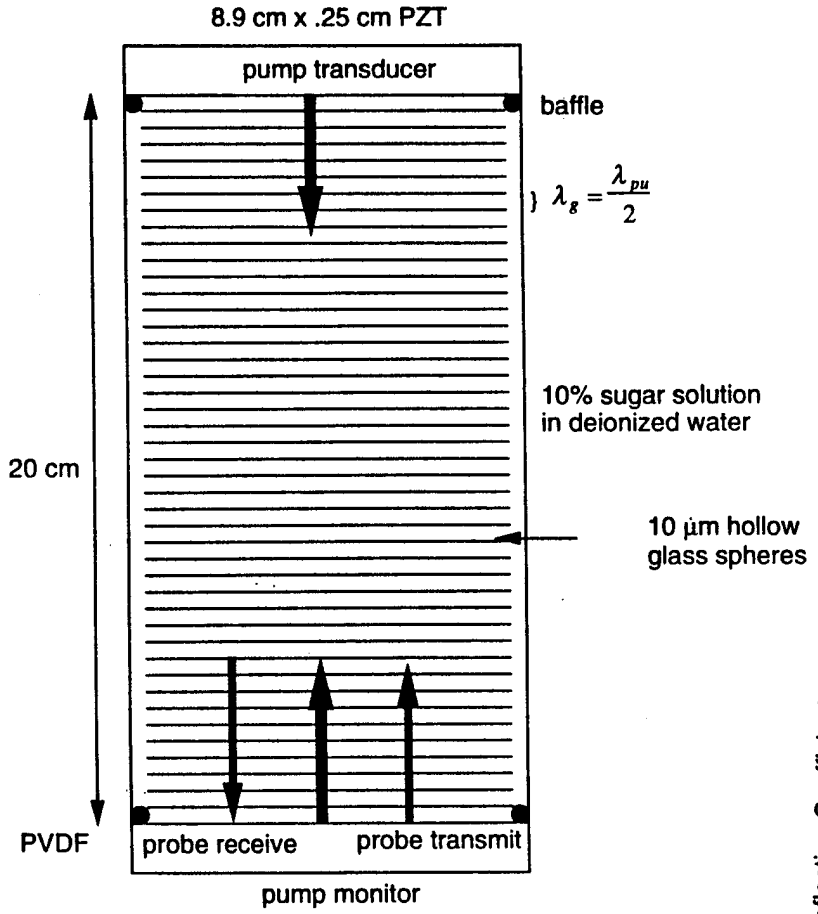

Figure 18

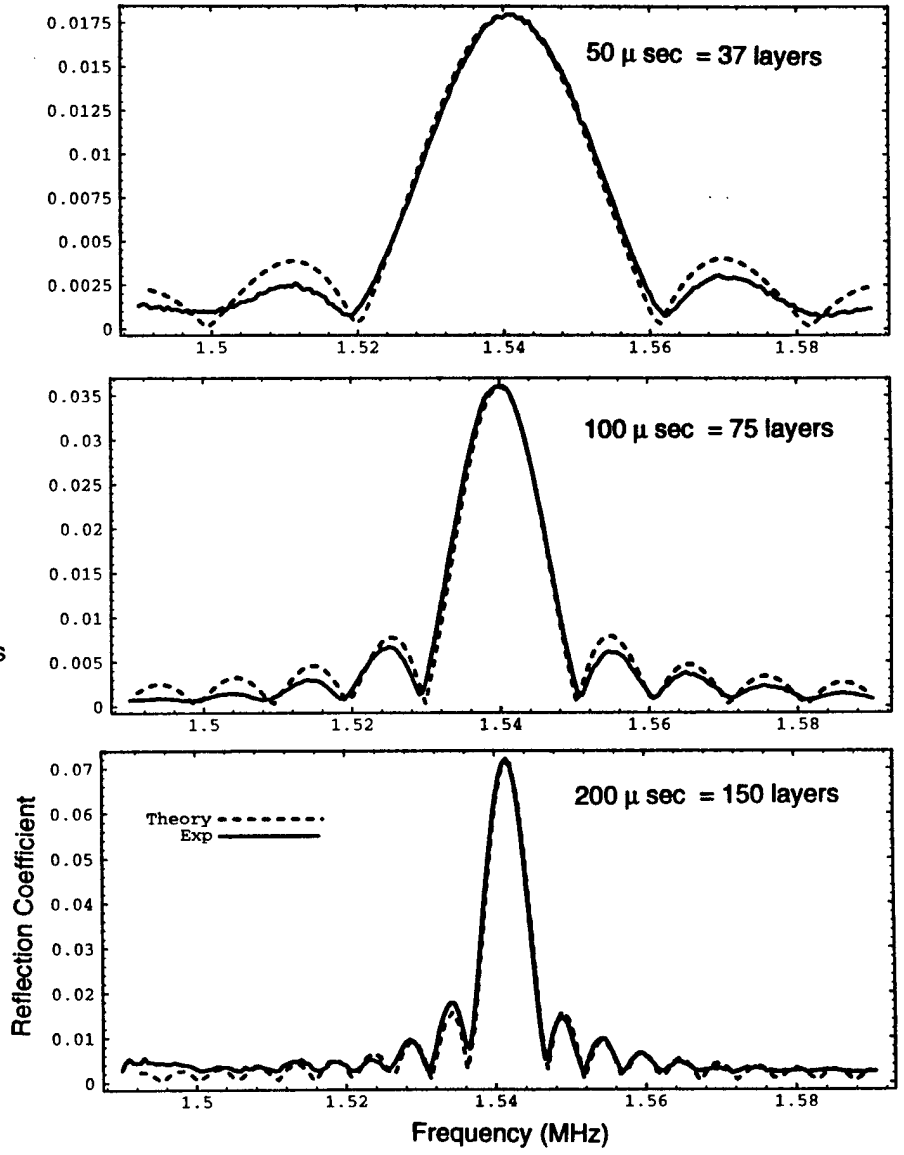

Figure 19

plotted in **Figure 19** for the Bragg peak centered at twice the pump frequency. In each of the figures there is one adjustable parameter to facilitate the comparison: the magnitude of the reflectivity at the peak was adjusted to fit the theoretical comparison. In the future it should be possible to calibrate the system to give the absolute reflectivity and thereby acoustically infer the equilibrium volume fraction of suspended particles.

2. Transfer matrix analysis of the Bragg reflection amplitude.

The analysis of Simpson and Marston[J11] is based on a Born approximation which does not take into account the depletion of the probe wave as it propagates through the grating. That approximation is limited to small values of the Bragg reflectivity. In anticipation of experiments where that assumption will breakdown, Kwiatkowski has implemented a transfer matrix calculation of the Bragg reflection amplitude. For weak or small gratings, the results based on the Born approximation are recovered but there are significant differences when the number of layers is large. The transfer matrix prediction saturates with a maximum reflectivity of unity unlike the (incorrect) Born predictions.

D. Supplemental research: Light scattering and sonoluminescence.

During the period under review, our experimental and theoretical research on a sequence of complicated optical caustics was published.[J1-3] The caustics are the result of light internally reflected two or more times within acoustically levitated oblate drops.

During summer semester of 1994, Mark Marr-Lyon performed exploratory observations of single bubble sonoluminescence (SBSL). The type of acoustic levitator used operated at 23 kHz and was a copy of the design developed for the levitation of large bubbles [Asaki, Marston, and Trinh, J. Acoust. Soc. Am. *93* , 706-13 (1993); Asaki and Marston, J. Acoust. Soc. Am. *96*, 3096-9 (1994) and *97*, 2138-43 (1995) and J. Fluid Mech. (accepted for publication)]. Short pulse SBSL optical signatures were recorded.[P1] A search for effects of a superposed static magnetic field on SBSL was inconclusive with the equipment available at that time.

In related research Marston investigated the theory of the lowest frequency modes of a cavity in water such as formed by an SBSL bubble. The question of interest is the following: Why does the reported SBSL spectrum fail to show any clear signatures of the cavity modes? In addition to the transient nature of the cavity and associated large velocity of the cavity walls, a tentative result of Marston's numerical analysis is that the quality factor or Q of bubble TE modes is small. This is in contrast to the case for drops of water where light may be trapped inside by internal reflection but is consistent with light scattering theory for bubbles, recently reviewed for bubbles by Stroud and Marston.[B1]

II. PERSONNEL

The following persons participated in the research.

Graduate students

1. G. Kaduchak: Completed Ph.D. degree in August 1994 pertaining to high-frequency and transient scattering by elastic shells in water. (Kaduchak is currently in a postdoctoral position at the Advanced Sonar Division of ARL, Univ. of Texas.)

2. J. S. Stroud: Completed Ph.D. degree in May 1995 on acoustic fluctuations and twinkling exponents due to the reflection by randomly curved surfaces. (Stroud is currently in a postdoctoral position at the Radiology Department of the Univ. of Cincinnati College of Medicine.)

3. S. F. Morse: Ph.D. candidate working on transient scattering.

4. K. Gipson: Ph.D. candidate working on scattering related problems. (Position facilitated by AASERT augmentation.)

5. C. Kwiatkowski: Ph.D. candidate working on ultrasonic four-wave mixing mediated by particle suspensions. (Position facilitated by AASERT augmentation.)

6. D. Ermer: In the summer semester of 1994 Ermer completed an M.S. degree project demonstrating the EMAT excitation of torsional and edge waves on a plate.

7. M. Marr-Lyon: In the summer semester of 1994, Marr-Lyon explored some aspects of single bubble sonoluminescence.

Other personnel

1. P. L. Marston: Principal investigator

2. D. B. Thiessen: Postdoctoral associate (principally supported by other ONR and NASA grants) who has improved our scientific and computational capabilities pertaining to this grant.

3. Z. Feng: Visiting Scientist from the Nanjing Research Institute who (while not directly supported by this grant) has improved our computational capabilities.

III. BIBLIOGRAPHY OF PUBLICATIONS AND REPORTS FOR GRANT N00014-92-J-1600

Research publications, pending publications, dissertations, technical and internal reports, reports of related previous work, and abstracted oral presentations are listed below according to category.

Code J: Refereed Journal Publications.

J1. G. Kaduchak, P. L. Marston, and H. J. Simpson, "E_6 diffraction catastrophe of the primary rainbow of oblate water drops: Observation with white light and laser illumination," Applied Optics **33**, 4691-4696 + 4961 (color plate) (1994).

J2. G. Kaduchak and P. L. Marston, "Hyperbolic umbilic and E_6 diffraction catastrophes associated with the secondary rainbow of oblate water drops: Observations with laser illumination," Applied Optics **33**, 4697-4701 (1994).

J3. P. L. Marston and G. Kaduchak, "Generalized rainbows and unfolded glories of oblate drops: Organization of multiple internal reflections and extension of cusps into Alexander's dark band," Applied Optics **33**, 4702-4713 (1994).

J4. P. L. Marston, "Leaky waves on curved scatterers: I. Fresnel width of coupling regions and elliptical Fresnel patches," J. Acoust. Soc. Am. **96**, 1893-98 (1994).

J5. K. L. Williams, J. S. Stroud, and P. L. Marston, "High frequency forward scattering from Gaussian spectrum, pressure release, corrugated surfaces. I: Catastrophe theory modeling," J. Acoust. Soc. Am. **96**, 1687-1702 (1994) (K. L. Williams supported by other ONR resources; J. S. Stroud supported by subcontract 721569 from University of Washington in that work.)

J6. G. Kaduchak, D. H. Hughes, and P. L. Marston, "Enhancement of the backscattering of high-frequency tone bursts by thin spherical shells associated with a backwards wave: Observations and ray approximation," J. Acoust. Soc. Am. **96**, 3704-3714 (1994).

J7. P. L. Marston and N. H. Sun, "Backscattering near the coincidence frequency of a thin cylindrical shell: Surface wave properties from elasticity theory and an approximate ray synthesis," J. Acoust. Soc. Am. **97**, 777-783 (1995).

J8. T. J. Matula and P. L. Marston, "Energy branching of a subsonic flexural wave on a plate at an air-water interface. I: Observation of the wave field near the interface and near the plate," J. Acoust. Soc. Am. **97**, 1389-1398 (1995).

J9. G. Kaduchak, C. S. Kwiatkowski, and P. L. Marston, "Measurement and interpretation of the impulse response for backscattering by a thin spherical shell using a broad-bandwidth source that is nearly acoustically transparent," J. Acoust. Soc. Am. **97**, 2699-2708 (1995).

J10. P. L. Marston, "Leaky waves on weakly-curved scatterers: II. Convolution formulation for two-dimensional high-frequency scattering," J. Acoust. Soc. Am. **97**, 34-41 (1995).

J11. H. J. Simpson and P. L. Marston, "Ultrasonic four-wave mixing mediated by an aqueous suspension of microspheres: Theoretical steady-state properties," J. Acoust. Soc. Am. (accepted for publication).

The following items listed in previous reports are not yet published:

J12. P. L. Marston, "Variable phase coupling coefficient for leaky waves on spheres and cylinders from resonance scattering theory," Wave Motion (accepted for publication).

J13. G. Kaduchak and P. L. Marston, "Traveling-wave decomposition of surface displacements associated with scattering by a cylindrical shell: Numerical evaluation displaying guided forward and backward wave properties," submitted to J. Acoust. Soc. Am.

Code B: Chapters in Books.

B1. J. S. Stroud and P. L. Marston, "Transient Bubble Oscillations Associated with the Underwater Noise of Rain Detected Optically and Some Properties of Light Scattered by

Bubbles," in *Bubble Dynamics and Interface Phenomena,* J. R. Blake *et al.* (eds.) (Kluwer, Dordrecht, 1994) pp. 161-169.

The following items listed in previous reports are not yet published:

B2. P. L. Marston, "Introductory Chapter—Ultrasonics, Quantum Acoustics, and Physical Effects of Sound," submitted to *Handbook of Acoustics* (John Wiley Press).

B3. P. L. Marston, "Quantitative Ray Methods for Scattering," submitted to *Handbook of Acoustics* (John Wiley Press).

Code T: Theses, Dissertations, Technical Reports, or Other Reports.

T1. G. Kaduchak, "Mode Threshold and Transient Scattering Processes for High Frequency Scattering of Sound by Elastic Shells in Water," Ph.D. dissertation, Department of Physics, Washington State University (1994), 214 pages [abstract published in J. Acoust. Soc. Am. **97**, 1345 (1995)].

T2. J. S. Stroud, "Twinkling of underwater sound reflected by one realization from a Gaussian spectrum population of corrugated surfaces" experiments and comparisons with a catastrophe theory approximation," Ph.D. dissertation, Department of Physics, Washington State University (1995), 260 pages. (Partially supported by ONR subcontract 721569 from Univ. of Washington.)

T3. P. L. Marston, "Scattering and radiation of high frequency sound in water by elastic objects, particle suspensions, and curved surfaces," (Annual Summary Report for N00014-92-J-1600 issued July 1994) DTIC Accession No. AD-A283 093, 46 pages.

Code P: Papers In Conference Proceedings.

P1. *Invited:* P. L. Marston, "Drops and Bubbles: Experimental Aspects," in "Proceeding of the 1994 Physical Acoustics Summer School," Vol. 1 (p. 48-104) and Vol. 2 (146 pages).

P2. *Invited:* P. L. Marston, D. H. Hughes, G. Kaduchak, and T. J. Matula, "High-frequency radiation and scattering processes for shells and plates in water: Backwards waves, coincidence enhancements, and transition radiation," in Third International Congress on Air- and Structure-Borne Sound and Vibration, edited by M. J. Crocker (International Scientific Pub., Auburn AL., 1994) pp. 1573-80 (See T3 for a manuscript copy.)

Code I: Internal Reports.

I1. D. R. Ermer, "Torsional, Edge, and Lamb Wave Excitation on a Plate in Air using an EMAT: An Experimental Investigation," M.S. degree project report, Physics Dept., Washington State University (1994).

Code M: Oral Presentations at Professional Meetings. Presentations at meetings having published proceedings are listed in code P (above). Unless otherwise noted presentations listed below were at national meetings of the Acoustical Society of America and abstracts were published.

M1. P. L. Marston, "Merging of launching or detachment points of weakly damped leaky waves on S-shaped surfaces and complex launching or detachment points," J. Acoust. Soc. Am. **95**, 2804 (1994).

M2. P. L. Marston, "Enhancement of the total scattering cross section near the coincidence frequency of thin shells," J. Acoust. Soc. Am. **95**, 2804 (1994).

M3. T. J. Matula and P. L. Marston, "Reflection of a subsonic flexural wave on a plate at an air-water interface and far-field observations of the transition radiation in water," J. Acoust. Soc. Am. **95**, 2972 (1994).

M4. P. L. Marston, "Symmetry and axial focusing in backscattering by elastic objects in water," J. Acoust. Soc. Am. **95**, 2999 (1994).

M5. S. G. Kargl and P. L. Marston, "Coupling coefficient for leaky waves on thick spherical shells from elasticity theory," J. Acoust. Soc. Am. **95**, 3001 (1994).

M6. *Invited:* K. L. Williams, J. S. Stroud, and P. L. Marston, "High frequency acoustic (scalar field) forward scattering from Gaussian spectrum, pressure release, corrugated surfaces producing clusters of caustics: Catastrophe theory modeling and experimental comparisons," URSI (International Union of Radio Science) Meeting Program (1994) p. 308.

M7. P. L. Marston, G. Kaduchak, and H. J. Simpson, "Diffraction catastrophes, lips events, and the unfolding of glory scattering by dielectric spheroids: analysis and observations," URSI (International Union of Radio Science) Meeting Program (1994) p. 113.

M8. *Invited:* P. L. Marston, G. Kaduchak, and D. H. Hughes, "Backscattering enhancements and the impulse response of shells: Observations and ray theory," J. Acoust. Soc. Am. **96**, 3304 (1994).

M9. G. Kaduchak and P. L. Marston, "Impulse response of thin shells: source development, analysis of the bipolar specular contribution, and computations showing the effect of water on the inside of the shell," J. Acoust. Soc. Am. **96**, 3324 (1994).

M10. K. Gipson and P. L. Marston, "Retroreflective backscattering of ultrasound due to Rayleigh waves on an elastic solid rectangular parallelepiped," J. Acoust. Soc. Am. **96**, 3325 (1994).

M11. J. S. Stroud, P. L. Marston, and K. L. Williams, "High-frequency forward scattering from Gaussian spectrum, pressure release, corrugated surfaces: Measurements of twinkling exponents and the dependence of the second moment on distance from surface and pulse length," J. Acoust. Soc. Am. **96**, 3231 (1994).

M12. P. L. Marston and S. F. Morse, "Pressure impulse response measurements for elastic scatterers in water and regulation of the source spectrum," J. Acoust. Soc. Am. **97**, 3239 (1995).

M13. P. L. Marston, "Variable phase coupling coefficient for leaky waves from resonance scattering theory and physical aspects of background contributions," J. Acoust. Soc. Am. **97**, 3283 (1995).

M14. C. S. Kwiatkowski and P. L. Marston, "Collinear ultrasonic four-wave mixing mediated by a suspension," J. Acoust. Soc. Am. **97**, 3327 (1995).

IV. DISTRIBUTION LIST
UNDER GRANT N00014-92-J-1600
ANNUAL SUMMARY REPORT

DR LOGAN E HARGROVE — 3 COPIES
OFFICE OF NAVAL RESEARCH
ONR 312
800 NORTH QUINCY STREET
ARLINGTON VA 22217-5660

DEFENSE TECHNICAL INFORMATION CENTER — 2 COPIES
BUILDING 5 CAMERON STATION
ALEXANDRIA VA 22314

ADMINISTRATIVE GRANTS OFFICER — 2 COPIES
OFFICE OF NAVAL RESEARCH
RESIDENT REPRESENTATIVE N63374
UNIV OF WASHINGTON UNIV DISTRICT
RM 410 1107 NE 45TH ST
SEATTLE WA 98105-4631

NAVAL RESEARCH LABORATORY
TECHNICAL LIBRARY CODE 5226
4555 OVERLOOK AVENUE SW
WASHINGTON DC 20375-5320

NAVAL POSTGRADUATE SCHOOL
TECHNICAL LIBRARY CODE 0212
MONTEREY CA 93943

NAVAL SURFACE WARFARE CENTER
COASTAL SYSTEMS STATION
TECHNICAL LIBRARY
PANAMA CITY FL 32407-5000

SUPPLEMENTAL DISTRIBUTION TO RESEARCH PARTICIPANTS AND TO OTHERS COUPLED WITH THE PROGRAM (1 COPY EACH)

G KADUCHAK
APPLIED RESEARCH LABORATORY
ADVANCED SONAR DEPT N330
UNIVERSITY OF TEXAS AT AUSTIN
PO BOX 8029
AUSTIN TX 78713-8029

J S STROUD
UNIVOF CINCINNATI COLLEGE OF MEDICINE
DEPT OF RADIOLOGY
231 BETHESDA AVE E560 MSB
PO BOX 670579
CINCINNATI OH 45267-0579

D H HUGHES
NAVAL RESEARCH LAB CODE 7136
4555 OVERLOOK AVE SW
WASHINGTON DC 20375-5350

H J SIMPSON
NAVAL RESEARCH LAB CODE 7136
4555 OVERLOOK AVE SW
WASHINGTON DC 20375-5350

T J MATULA
APPLIED PHYSICS LABORATORY
UNIVERSITY OF WASHINGTON
SEATTLE WA 98105-6698

K L WILLIAMS
APPLIED PHYSICS LABORATORY
UNIVERSITY OF WASHINGTON
SEATTLE WA 98105-6698

K GIPSON
C KWIATKOWSKI
S F MORSE
D B THIESSEN
DEPARTMENT OF PHYSICS
WASHINGTON STATE UNIVERSITY
PULLMAN WA 99164-2814

T J ASAKI
GROUP MST-10
LOS ALAMOS NATIONAL
LABORATORY
LOS ALAMOS NM 87545

W PATRICK ARNOTT
ATMOSPHERIC SCIENCES CENTER
DESERT RESEARCH INSTITUTE
P O BOX 60220
RENO NV 89506

C K FREDERICKSON
PHYSICS DEPARTMENT
UNIV OF CENTRAL ARKANSAS
CONWAY AR 72035

S G KARGL
APPLIED PHYSICS LABORATORY
UNIVERSITY OF WASHINGTON
SEATTLE WA 98105-6698

C E DEAN
PHYSICS DEPT
GEORGIA SOUTHERN UNIVERSITY
LANDRUM BOX 8031
STATESBORO GA 30460

OTHER SUPPLEMENTAL DISTRIBUTION (1 COPY EACH)

D G TODOROFF
COASTAL SYSTEMS STATION
PANAMA CITY FL 32407-5000

RAYMOND LIM
COASTAL SYSTEMS STATION
PANAMA CITY FL 32407-5000

F M PESTORIUS DIRECTOR
APPLIED RESEARCH LABORATORIES
UNIVERSITY OF TEXAS AT AUSTIN
AUSTIN TX 78713-8029

ROGER H HACKMAN
LOCKHEED PALO ALTO RES LABS
PALO ALTO CA 94304-1191

ANTHONY A ATCHLEY
DEPARTMENT OF PHYSICS
CODE PH/AY
NAVAL POSTGRADUATE SCHOOL
MONTEREY CA 94943-5000

YVES H BEETHELOT
SCHOOL OF MECHANICAL
ENGINEERING
GEORGIA INSTITUTE OF
TECHNOLOGY
ATLANTA GA 30332

ALLAN D PIERCE
DEPT OF AEROSPACE & MECH ENGR
BOSTON UNIVERSITY
110 CUMMINGTON STREET
BOSTON MA 02215

C M LOEFFLER
APPLIED RESEARCH LABORATORIES
UNIVERSITY OF TEXAS AT AUSTIN
AUSTIN TX 78713-8029

J W DICKEY
CARERROCK DIVISION CODE 2704
NAVAL SURFACE WARFARE CENTER
BETHESDA MD 20084-5000

HENRY E BASS
DEPT OF PHYSICS AND ASTRONOMY
UNIVERSITY OF MISSISSIPPI
UNIVERSITY MS 386777

LAWRENCE A CRUM
APPLIED PHYSICS LABORATORY
UNIVERSITY OF WASHINGTON
1013 NE 40TH STREET
SEATTLE WA 98105-6698

MOISES LEVY
DEPARTMENT OF PHYSICS
UNIV OF WISCONSIN AT MILWAUKEE
MILWAUKEE WI 53201

MARK F HAMILTON
DEPT OF MECHANICAL ENGINEERING
UNIVERSITY OF TEXAS AT AUSTIN
AUSTIN TX 78712-1063

WALTER G MAYER
DEPARTMENT OF PHYSICS
GEORGETOWN UNIVERSITY
WASHINGTON DC 20057

WOLFGANG H SACHSE
THEORETICAL AND APPLIED MECHANICS
CORNELL UNIVERSITY
ITHACA NY 14853-1503

IRA DYER
DEPARTMENT OCEAN ENGINEERING
MASSACHUSETTS INST TECHNOLOGY
CAMBRIDGE MA 02139

STEVEN R BAKER
NAVAL POSTGRADUATE SCHOOL
DEPARTMENT OF PHYSICS CODE PH/BA
MONTEREY CA 93943-5004

TIMOTHY K STANTON
WOODS HOLE OCEANOGRAPHIC INST
WOODS HOLE MA 02543

ANDREA PROSPERETTI
DEPT OF MECHANICAL ENGINEERING
JOHNS HOPKINS UNIVERSITY
BALTIMORE MD 21218

ROBERT E APFEL
DEPT OF MECHANICAL ENGINEERING
YALE UNIVERSITY
NEW HAVEN CT 06520-2159

L B FELSEN
DEPT OF AEROSPACE & MECH ENGR
BOSTON UNIVERSITY
110 CUMMINGTON STREET
BOSTON MA 02215

LOUIS R DRAGONETTE
NAVAL RESEARCH LABORATORY
4555 OVERLOOK AVE SW
WASHINGTON DC 20375-5350

MICHAEL F WERBY
NRL CODE 7181
STENNIS SPACE CENTER
MS 39529

ANDREW N NORRIS
DEPT MECH AND AEROSP ENGR
RUTGERS UNIVERSITY
P O BOX 909
PISCATAWAY NJ 08855-0909